PERGAMON

International Journal of Multiphase Flow 24 (1998) 913–945

International Journal of Multiphase Flow

On the Lagrangian turbulent dispersion models based on the Langevin equation

Jacek Pozorski[a,*], Jean-Pierre Minier[b]

[a]*Institute of Fluid Flow Machinery, Polish Academy of Sciences, ul. Fiszera 14, 80952, Gdańsk, Poland*
[b]*Laboratoire National d'Hydraulique, Electricité de France, 6 quai Watier, 78400, Chatou, France*

Received 29 October 1997; received in revised form 20 May 1998

Abstract

A Lagrangian approach is used to describe turbulent two-phase particulate flows. Special attention focuses on a currently used model based on the Langevin equation with instantaneous relative velocity of fluid and particles. A detailed analysis of the model is performed and its drawbacks are discussed. Afterwards, a novel model for particle dispersion in homogeneous turbulence is proposed. It is built on physical arguments quite different from those underlying the previous model: rather than instantaneous relative velocities, averaged characteristics of the motion of solid–fluid particle pairs are considered. The new model accounts for both inertia and external force effects. It is validated by comparison with existing experimental data on particle dispersion in grid turbulence and with large-eddy simulations of homogeneous turbulence.

Keywords: Turbulent dispersion; Lagrangian approach; Inertia effect; Mean drift effect; Langevin equation

1. Introduction

Two-phase turbulent flows with particles ('particle' is here a generic term for both solid particles and liquid droplets) are common in the environmental science and engineering. There are two established ways of modelling these flows. In the 'two-fluid' (or Eulerian) approach both phases are treated as interacting and interpenetrating continua; a number of mean variables (such as velocity, turbulent kinetic energy, etc.) are selected separately for the two phases and Reynolds-averaged equations governing their evolution are solved. On the other hand, in the 'trajectory' (or Lagrangian) approach the dispersed phase is directly treated as an ensemble of many individual inclusions; the exact instantaneous equations governing particle

* Corresponding author. Fax.: +48 58 3416144; E-mail: jp@galia.imp.pg.gda.pl.

0301-9322/98/$19.00
PII: S0301-9322(98)00016-0

dynamics are replaced by modelled ones and mean quantities (velocity, concentration, turbulent kinetic energy) are obtained afterwards by ensemble averaging over a large number of particles. Advantages and drawbacks of the Eulerian and Lagrangian description have been discussed by Crowe (1982), Durst et al. (1984) and Stock (1996). Although the two approaches applied to dispersed turbulent flows are often presented as being fundamentally different, this is, in a way, misleading. The description is indeed made with different variables (Eulerian or Lagrangian) but the underlying models are often the same (cf. Simonin et al., 1993; Simonin, 1996).

1.1. Background

The starting point of the Lagrangian approach is the particle equation of motion (see Maxey and Riley, 1983; Gatignol, 1983). It contains several terms, but with the assumptions of heavy particles, $\rho_f \ll \rho_p$, and no rapid transients, the drag and buoyancy forces are shown to be dominant:

$$\frac{d\mathbf{x}_p}{dt} = \mathbf{v}_p, \quad \frac{d\mathbf{v}_p}{dt} = \frac{\mathbf{v}[\mathbf{x}_p(t), t] - \mathbf{v}_p}{\tau_p} + \mathbf{g} \tag{1}$$

Here, the drag term has been written using the particle relaxation (dynamic response) time

$$\tau_p = \frac{\rho_p}{\rho_f} \frac{4d}{3C_D|\mathbf{v} - \mathbf{v}_p|} \tag{2}$$

with the drag coefficient $C_D = C_D(Re_p)$ usually given by a semi-empirical formula written as a function of the particle relative Reynolds number (Clift et al., 1978).

As readily seen in (1), the driving fluid velocity $\mathbf{v}^*(t) = \mathbf{v}[\mathbf{x}_p(t), t]$, i.e. instantaneous velocities of successive fluid particles (F, cf. Fig. 1) that cross the solid particle (S) trajectory $\mathbf{x}_p(t)$, is a function of time only (henceforth variables denoted by an asterisk relate to the fluid 'seen' by the particles). So, the equation of motion can be used (in principle, at least) to compute the statistical characteristics of the particle velocity $\mathbf{v}_p$ as a function of the fluid velocity 'seen' $\mathbf{v}^*$. However, the main difficulty lies in the accurate prediction of $\mathbf{v}^*(t)$ in the general case of turbulent flow. The point is that the Reynolds averaging in fluid turbulence results in transport equations for the mean variables like mean velocity $\langle \mathbf{V} \rangle$, turbulent kinetic energy k, turbulent

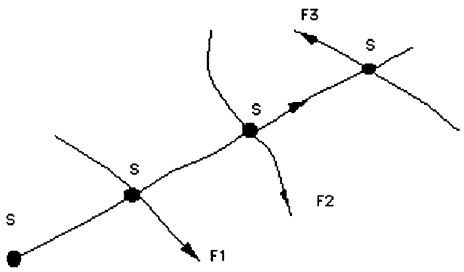

Fig. 1. Fluid element and particle paths.

energy dissipation rate ϵ, but during the averaging process, detailed information about instantaneous fluid structures is lost. In the Lagrangian approach to particle dispersion one has thus to somehow reconstruct instantaneous (or fluctuating, since mean values are given) fluid velocities from the averaged Navier–Stokes equations.

In order to develop stochastic models or schemes for the generation of $\mathbf{v}^*(t)$, one typically uses, together with particle parameters (such as τ_p), a few quantities derived from the fluid variables, like the Eulerian length scale L_E or the Lagrangian time scale T_L; based on simple dimensional arguments, these scales are estimated as $L_E = C_E k^{3/2}/\epsilon$ and $T_L = C_L k/\epsilon$ (C_E and C_L are experimental constants). The modelling of $\mathbf{v}^*(t)$ is complicated, because of two effects that cause the fluid element and particle trajectories to differ: first, particle inertia that induces a relative instantaneous motion of particles with regard to their fluid neighbourhood, and second, mean particle drift due to gravity.

In the case of stationary isotropic turbulence with no external force, particle inertia is the only relevant effect. Tchen (see Hinze, 1975) expressed the particle fluctuating velocity variance $\langle v_p^2(t)\rangle$ and velocity correlation function in terms of fluid characteristics, i.e. the fluid velocity variance σ_f^2, the fluid Lagrangian autocorrelation function $R_L(t)$ or its temporal integral (the Lagrangian timescale T_L); he stated that

$$\langle v_p^2(t)\rangle = \sigma_f^2 \frac{T_L/\tau_p}{1 + T_L/\tau_p}. \tag{3}$$

The ratio of characteristic timescales, T_L/τ_p, stands for the inertia parameter characterizing the influence of turbulence on the particle motion.

In a gravity field (or any external force field), there is a relative mean motion of heavy particles and the turbulent fluid neighbourhood; due to their free-fall velocity, $v_g = \langle v_p\rangle$, the particles continuously drift from one fluid element to another. Consequently, the fluid velocities 'seen' by the particles are usually less correlated than the Lagrangian fluid velocities and the dispersion coefficient decreases. The phenomenon (called 'crossing trajectory effect') can be characterized in terms of the nondimensional ratio of characteristic velocities $\xi = v_g/\sigma_f$. Csanady (1963) proposed expressions for the velocity correlation and the Lagrangian timescales of the fluid 'seen':

$$\begin{aligned} &R^*_{L(.)}(\Delta t) = \langle v^*_{(.)}(t) v^*_{(.)}(t+\Delta t)\rangle = \exp\left(-\frac{\Delta t}{T^*_{L(.)}}\right), \; T^*_{L(\parallel)} = \frac{T_L}{\sqrt{1+\beta^2\xi^2}}, \\ &T^*_{L(\perp)} = \frac{T_L}{\sqrt{1+4\beta^2\xi^2}} \end{aligned} \tag{4}$$

where $\beta = T_L/T_E = \sigma_f T_L/L_E$ and the subscript $(\cdot)$ denotes direction either parallel ($\parallel$) or perpendicular ($\perp$) to that of the external force.

1.2. Objective

In the present work, we will apply the Lagrangian approach to compute particle dispersion. We will consider dilute, or low-loading, two-phase flows containing spherical particles with the

one-way momentum coupling, i.e. flows where the influence of the dispersed phase on the carrying fluid (but not the inverse) can be neglected.

The aim of the present study is to analyse the consistency and the physical justification of the modelling steps, as well as to put forward a new dispersion model, based on conclusions from the analysis. In particular, the issue of the relative velocity of particle–fluid pair is found to be of primary importance for a sound model; that is why the modelling of the particle inertia and the mean drift effects is thoroughly examined. For this reason, particle dispersion is considered only for the case of isotropic stationary turbulence and the paper is not directly concerned with the comparison of performance of different models in practical situations.

The paper is organised as follows. Existing turbulent dispersion models are recalled in Section 2; the subsequent sections contain an original material. First, a detailed analysis of an often used two-step Langevin model is presented (Section 3). Then, a novel model for particle dispersion is proposed and discussed (Section 4); physical arguments behind this model are put forward. Next, results of numerical simulation of the dispersed phase are given (Section 5). The performance of the new model is examined by comparison with existing experimental data on particle dispersion in grid turbulence and with the outcome of a 'numerical experiment' (the large-eddy simulation). Finally, Section 6 is devoted to summary and conclusions.

2. Existing Models of Turbulent Diffusion and Dispersion

A common feature of most Lagrangian methods used to date is the decomposition of the driving fluid velocity into the mean and the fluctuating parts. The mean fluid velocity field results from the continuous phase computation and is interpolated at particle locations. Then, a Lagrangian model gives the fluctuating component. This decomposition is not necessarily the most convenient one and working with the instantaneous velocities is often better in the general case. However, in the present work, concerned with the homogeneous isotropic turbulence, in the reference frame moving with the constant mean velocity there is no difference between instantaneous and fluctuating velocities. Most Lagrangian models for two-phase flows follow a twin fluid particle along with the solid particle and the fluid velocities seen by the solid particle are derived from a two-step scheme. Therefore we start our presentation with the question of fluid diffusion before considering particle dispersion.

2.1. Models for fluid diffusion

Historically, the first method developed (Gosman and Ioannides 1981) was the eddy-life time (ELT). Its major feature is the sampling of the fluid particle fluctuating velocity in the Gaussian distribution of zero mean and a variance equal to the mean square turbulent velocity. The sampled velocity is kept constant during a time interval T corresponding to the typical timescale of the energy containing eddies. The drawbacks of the method are twofold: a resulting velocity correlation coefficient is linear (rather than exponential), and the velocity record for a fluid particle is discontinuous. The former disadvantage has been coped with by Ormancey (1984); he considered the time interval between subsequent velocity changes as an exponentially-distributed random variable (a Poisson process) with the mean value T.

To deal with the latter unphysical feature (discontinuous velocity records), a following stochastic differential equation has been proposed to model the behaviour of fluid velocities

$$\mathrm{d}v = v(t+\mathrm{d}t) - v(t) = -\frac{v}{T_\mathrm{L}}\mathrm{d}t + \sigma_\mathrm{f}\sqrt{\frac{2}{T_\mathrm{L}}}\mathrm{d}W. \tag{5}$$

Here, $\mathrm{d}W$ is the Wiener process (white noise); it is a stochastic process of zero mean, $\langle \mathrm{d}W\rangle = 0$, a variance equal to the time interval, $\langle(\mathrm{d}W)^2\rangle = \mathrm{d}t$, and delta-correlated in the time domain (Arnold, 1974; Schuss, 1980; Sobczyk, 1991). The above is the Langevin equation first proposed to model the Brownian motion; in that context, it represents the equation of motion of a small particle in surrounding fluid. The effect of collisions of the Brownian particle with fluid molecules is split in two contributions: a resistive drag term and a pure random term. For the case of fluid turbulence, such a division has been proposed based on different arguments (Minier and Pozorski 1997).

Obviously, since the above stochastic differential equation is to model the behaviour of fluid elements, it needs justification. First, it is generally accepted that velocity fluctuations are related to the large energetic scales in turbulent flow while acceleration fluctuations are governed by small-scale motions. Thus characteristic time scales for velocity and acceleration are quite different. If one considers time intervals corresponding to velocity changes of a fluid element, the acceleration is a rapidly fluctuating process and, under the assumption of Gaussianity, it can be seen as a white-noise process. Next, the Lagrangian velocity structure function, computed as the ensemble mean of Eq. (5) squared

$$D_\mathrm{L}(\mathrm{d}t) = \langle[v(t+\mathrm{d}t) - v(t)]^2\rangle = \langle(\mathrm{d}v)^2\rangle = \frac{2\sigma_\mathrm{f}^2}{T_\mathrm{L}}\mathrm{d}t \tag{6}$$

accords with the Kolmogorov theory (Monin and Yaglom 1971) that predicts the structure function in the inertia subrange ($\tau_\eta \ll \Delta t \ll T_\mathrm{L}$) to be linear with respect to the time interval, $D_\mathrm{L}(\Delta t) = C_0\langle\epsilon\rangle\Delta t$. Hence

$$T_\mathrm{L} = \frac{4}{3C_0}\frac{k}{\langle\epsilon\rangle}. \tag{7}$$

Formula (7) is valid for stationary turbulence; we add here for the sake of completeness that the Langevin model has recently been formulated in terms of instantaneous velocities and extended to the general case of non-homogeneous turbulence with mean pressure gradients (Pope, 1994):

$$\mathrm{d}U_i = -\frac{1}{\rho_\mathrm{f}}\frac{\partial\langle p\rangle}{\partial x_i}\mathrm{d}t - \left(\frac{1}{2}+\frac{3}{4}C_0\right)\frac{\langle\epsilon\rangle}{k}(U_i - \langle U_i\rangle)\mathrm{d}t + \sqrt{C_0\langle\epsilon\rangle}\ \mathrm{d}W_i. \tag{8}$$

Some advantages of such a formulation, as compared to models working with fluctuating velocities, can be stated: it is physically consistent (no need to use mean variables computed from an Eulerian code) and there are no spurious drifts in non-homogeneous case (MacInnes and Bracco 1992).

As velocities of fluid particles are to be generated in the numerical simulation at each time step, a discrete version of Eq. (5) is needed. The simplest discretisation writes:

$$v^{n+1} = av^n + be^n, \tag{9}$$

where e is a random number taken from the standard Gaussian distribution ($\langle e\rangle = 0$, $\langle e^2\rangle = 1$), denoted by $e \in \mathcal{N}(0,1)$. It is worth emphasizing that this simple relation embodies the main physical idea of the model: given the value of the fluid particle velocity at a certain time t^n, the velocity at the next time step, $t^{n+1} = t^n + \Delta t$, is evaluated as the sum of a deterministic term which represents the 'memory' of the previous velocity and a random term which accounts for the acceleration fluctuations. To find the coefficients a and b, we multiply the above equation by v^n, v^{n+1}, respectively, and take the ensemble mean to obtain:

$$\begin{aligned} a &= \frac{\langle v^n v^{n+1}\rangle}{\langle (v^n)^2\rangle} = R_{\mathrm{L}}(\Delta t) = \exp\left(-\frac{\Delta t}{T_{\mathrm{L}}}\right), \\ b^2 &= [\langle v^{n+1} v^{n+1}\rangle - a^2\langle (v^n)^2\rangle] = \sigma_{\mathrm{f}}^2(1-a^2). \end{aligned} \tag{10}$$

Here, we made use of the exponential correlation of the process and of its stationarity, $\langle (v^n)^2\rangle = \sigma_{\mathrm{f}}^2$.

Eq. (9) can be thought of as a numerical scheme for (5). Indeed, the differential equation is easily retrieved by taking the limit $\Delta t \to 0$ and using a property of the Wiener process, $e^n\sqrt{\Delta t} \to \mathrm{d}W$. Berlemont et al. (1990) proposed a heuristic generalisation, in a sense, of the discrete Langevin Eq. (9). They used autoregressive stochastic process so as to allow any form of the fluid velocity correlation. It is worth mentioning, however, that the present Langevin model follows a different philosophy. It is not a discrete-only proposal derived to reproduce a given correlation function, but rather a continuous model based on a stochastic differential equation; only a timescale is input and the actual form of the autocorrelation is a result of the model.

2.2. Models for particle dispersion

For inclusions such as solid particles the situation is more complicated due to the effects of particle inertia and external forces such as gravity. As already mentioned, in the Lagrangian framework the problem is to simulate the fluid turbulent velocities seen by particles along their trajectories. The particle P and the fluid element (fluid particle) F whose positions coincide at some time instant will generally separate during the next time interval. Even if we are able to somehow model instantaneous fluid particle velocities (using the methods that have just been presented), we still have to estimate the velocity of another fluid particle F' given the velocity record of particle F (see Fig. 2). The methods proposed for fluid diffusion have to be extended in order to account for this separation. The possible extensions are twofold: the new driving velocity of F' at t^{n+1} is generated either directly from the velocity of F at t^n or through a two-step approach.

Let us start with the direct approaches. First, the ELT method is readily extended to the particle dispersion case by a modification of T, taken now as the smaller of the eddy-life time and the eddy-interaction time (Gosman and Ioannides, 1981; Graham, 1996). Second, in the direct Langevin model (Perkins et al., 1991) the new fluid velocity $\mathbf{v}_{\mathrm{f}'}^{n+1}$ of the fluid particle F' at the time t^{n+1} is written as a function of the velocity of the fluid particle F at the time t^n

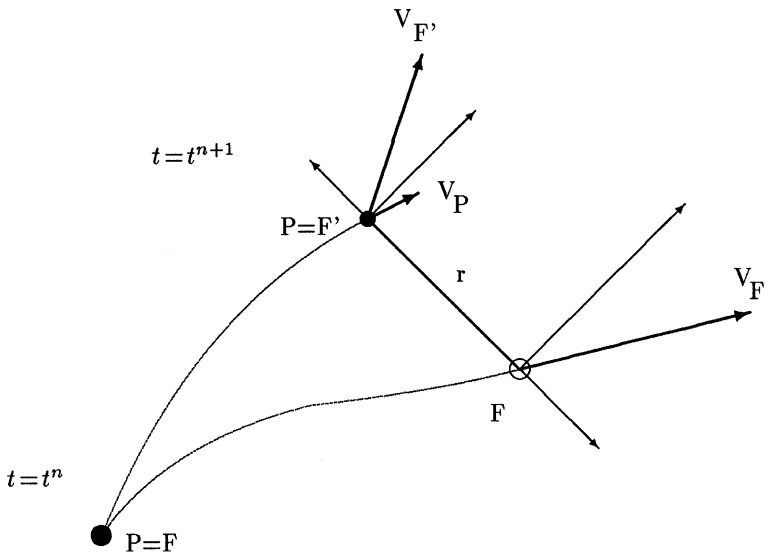

Fig. 2. Solid–fluid pair.

(see Fig. 2).

$$\mathbf{v}_{\mathrm{f}'}^{n+1} = a\mathbf{v}_{\mathrm{f}}^{n} + b\mathbf{e}^{n}, \tag{11}$$

$$a = \exp\left(\frac{\Delta t}{T_{\mathrm{L}}^{*}}\right), \quad b = \sigma_{\mathrm{f}}\sqrt{1-a^{2}}, \quad \mathbf{e} \in \mathcal{N}(0,1). \tag{12}$$

In this method, the Lagrangian integral timescale of the fluid seen by the solid particles, T_{L}^{*}, is an unknown parameter which must be given beforehand. One possibility is to use Csanady's expression (4).

On the other hand, two-step approaches (see the scheme in Fig. 2) consist of the so-called Lagrangian step (the same as in turbulent diffusion models) where the velocity of the same fluid particle F at the next time step t^{n+1} is computed, and a subsequent Eulerian step which generates the new velocity of F' from that of F at t^{n+1}. As already shown, the Lagrangian step consists in [here the notation differs slightly from that of Eq. (9)]:

$$\mathbf{v}_{\mathrm{L}} = \mathbf{v}_{\mathrm{f}}^{n+1} = a_{\mathrm{L}}\mathbf{v}_{\mathrm{f}}^{n} + b_{\mathrm{L}}\mathbf{e}_{\mathrm{L}}^{n}, \tag{13}$$

with

$$a_{\mathrm{L}} = \exp\left(-\frac{\Delta t}{T_{\mathrm{L}}}\right), \quad b_{\mathrm{L}} = \sigma_{\mathrm{f}}\sqrt{1-a_{\mathrm{L}}^{2}}, \quad \mathbf{e}_{\mathrm{L}}^{n} \in \mathcal{N}(0,1). \tag{14}$$

A very tempting idea is to apply a similar concept to the second step, substituting time variables by their spatial equivalents (Zhuang et al., 1989; Zhou and Leschziner, 1991; Minier and Simonin, 1992; Lu et al., 1993). The Eulerian (spatial) step writes:

$$v_i^{n+1} = v_{\mathrm{f}'i}^{n+1} = a_{\mathrm{E}(.)} v_{\mathrm{L}i} + b_{\mathrm{E}(.)} e_{\mathrm{E}i}^{n+1}, \tag{15}$$

with

$$a_{\mathrm{E}(.)} = \exp\left(-\frac{r}{L_{\mathrm{E}(.)}}\right), \quad b_{\mathrm{E}(.)} = \sigma_{\mathrm{f}}\sqrt{1 - a_{\mathrm{E}(.)}^2}, \quad \mathbf{e}_{\mathrm{E}}^{n+1} \in \mathcal{N}(0, 1). \tag{16}$$

Due to anisotropy of space correlations, these equations are written in the local coordinate system where the vector Ox points from the fluid particle to the solid particle location (Fig. 2); so, the subscript $(\cdot)$ denotes $(\parallel)$ for $i = 1$ and $(\perp)$ for $i = 2, 3$ [cf. also Eq. (4)], respectively. To be consistent with the properties of Markov chains, exponential functions are used for the Eulerian correlations, and r

$$r = |\mathbf{v}^n - \mathbf{v}_{\mathrm{p}}^n| \Delta t \tag{17}$$

stands for the relative distance of the fluid and solid particle at the time t^{n+1}.

3. Analysis of the Langevin Model with Instantaneous Relative Velocity

The two-step particle dispersion model from the previous section, Eqs. (13) and (15), called for brevity the Langevin model with instantaneous relative velocity (LIV), will now be examined. Such an analysis seems worthwhile, because the LIV model is in frequent use nowadays (Berlemont et al., 1990; Burry and Bergeles, 1993; Lu et al., 1993; Ormancey, 1984; Sommerfeld et al., 1993; Yvergniaux, 1990; Zhuang et al., 1989) and its drawbacks have not yet been discussed in the literature. The idea of the model is an individual treatment of all fluid-solid particle pairs; namely, all relative distances between fluid and dense particles are calculated from their simulated instantaneous velocities. A number of characteristic features of the LIV model will be discussed in the sequel. Numerical simulations will illustrate and support the theoretical considerations. We start the analysis by considering the case without an external force field, $g = 0$. The effect of gravity will be accounted for in Section 3.5.

3.1. Differential limit of the spatial step

It was stated in the previous section that for the Lagrangian step, in the limit $\Delta t \to 0$ the discrete Eq. (9) becomes the differential Eq. (5) that is physically justified. Now, for the Eulerian (spatial) step, the differential equation corresponding to Eq. (15) writes

$$\mathrm{d}v = -\frac{v}{L_{\mathrm{E}}}\mathrm{d}r + \sigma_{\mathrm{f}}\sqrt{\frac{2}{L_{\mathrm{E}}}}\mathrm{d}W. \tag{18}$$

The velocity differences over distances Δr that lie in the inertia range, $\eta \ll \Delta r \ll L_{\mathrm{E}}$, are given by $\Delta v_{\mathrm{r}} = v(r + \Delta r) - v(r)$. They are Gaussian random variables whose first three moments are:

$$\langle \Delta v_r \rangle = 0, \quad \langle (\Delta v_r)^2 \rangle = \frac{2\sigma_f^2}{L_E} \Delta r, \quad \langle (\Delta v_r)^3 \rangle = 0. \tag{19}$$

On the other hand, the Kolmogorov hypothesis yields the following scaling laws for the velocity structure function:

$$\langle \Delta v_r \rangle = 0, \quad \langle (\Delta v_r)^2 \rangle = (\langle \epsilon \rangle \Delta r)^{2/3}, \quad \langle (\Delta v_r)^3 \rangle = \langle \epsilon \rangle \Delta r. \tag{20}$$

We can see that the Langevin equation model respects neither the famous two-third power law scaling of the characteristic eddy velocities in the inertia range nor the third order moment. Yet, the skewness has a clear significance in turbulence theory where it is related to energy transfer from larger to smaller scales which is not present here. Thus, contrary to (5), Eq. (18) has less physical support. On the other hand, note that the above-listed limitations not necessarily invalidate a Langevin-type equation of the form (18), but rather the present formulation with a linear drift and a constant diffusion coefficient.

3.2. Effect of finite correlation length

In the methods originally proposed by Zhuang et al. (1989) and Berlemont et al. (1990), the same fluid particle accompanying a dense particle is followed during several time steps until the distance between them becomes greater than a certain cutoff length L_D, usually of the order of L_E (see Fig. 3a). A physical argument behind the cutoff length concept is that the velocities of two fluid particles separated by a distance greater than L_D are practically uncorrelated. Yet, the turbulent flow should be considered as an ensemble of structures whose dimensions belong to the whole spectrum rather than a set of eddies of a typical size L_D.

In the Langevin equation model proposed for example by Minier and Simonin (1992), no decorrelation length is introduced since it is believed that the crossing-trajectory effect is already simulated by the Eulerian step which actually induces a loss of correlation and should not be supplemented with a cutoff parameter. Given a particle P and a fluid particle F whose locations coincide at time t^n, they will usually separate at t^{n+1}. The two-step approach requires the generation of the velocity of the new fluid neighbour F'. For the next time step, from t^{n+1} to t^{n+2}, it is also possible to derive the next fluid velocity $\mathbf{v}_{f'}^{n+2}$ from $\mathbf{v}_{f'}^{n+2}$ instead of going back to F and deriving it from $\mathbf{v}_f^{n+2}$. It seems that the first choice is more reasonable

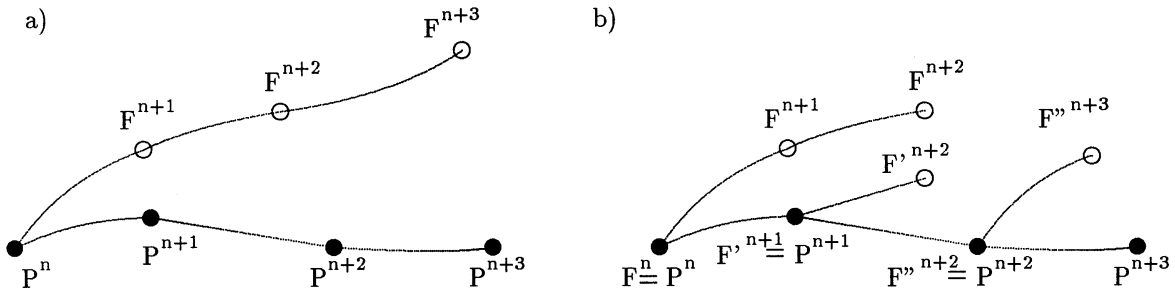

Fig. 3. Particle dispersion based on the instantaneous relative velocity: (a) classical method; (b) method used in the simulation.

since, by changing the twin fluid particle at each time step (see Fig. 3b), we have to span smaller distances for which the method is more reliable.

The value of L_D is often considered to be a free parameter of the LIV model, thus enabling to obtain the best fit of the simulated dispersion results to the experimental data. Ormancey (1984) and Yvergniaux (1990) took $L_D = L_{E(\perp)}$, whereas $L_D = 1.5L_{E(\perp)}$ was the value used by Zhuang et al. (1989) and Berlemont et al. (1990).

The introduction of a finite correlation length means that the tail of the correlation $R_E(r)$ is disregarded for distances $r \geq L_D$. This implicitly introduces a modified correlation coefficient $\hat{R}_E(r)$ and leads to an artificial decrease of the simulated lengthscale. In order to measure this effect, consider, for the sake of simplicity, a one-dimensional case; it is, in fact, equivalent to a three-dimensional case with $L_{E(\parallel)} = L_{E(\perp)}$. A formula used to simulate spatial correlations, proposed in the cited papers, writes:

$$\hat{R}_E(r) = \begin{cases} R_E(r) & \text{for} \quad r \leq L_D \\ 0 & \text{for} \quad r > L_D. \end{cases} \tag{21}$$

The Eulerian spatial velocity correlation coefficient R_E may take the exponential form:

$$R_E(r) = \exp\left(-\frac{r}{L_E}\right) \tag{22}$$

or can be constant: $R_E(r) = 1$ (spatial equivalent of the ELT method). Let us calculate the spatial correlation which is actually simulated:

$$R_E^{(sim)}(r) = \frac{1}{\sigma_f^2}\overline{\langle v(\rho)v(\rho + r)\rangle}. \tag{23}$$

Here, the angular brackets denote the ensemble mean over all realizations for a given initial position ρ, whereas an overbar stands for the average over all values of ρ. Because of periodicity, it is sufficient to consider the values of ρ from the interval $[0, L_D]$. So we write:

$$R_E^{(sim)}(r) = \frac{1}{\sigma_f^2 L_D}\int_0^{L_D} \langle v(\rho)v(\rho + r)\rangle \mathrm{d}\rho = \frac{1}{\sigma_f^2 L_D}\left[\int_0^{L_D - r} + \int_{L_D - r}^{L_D}\right]\langle v(\rho)v(\rho + r)\rangle \mathrm{d}\rho \tag{24}$$

for $r < L_D$; obviously, $R_E^{(sim)}(r) = 0$ for $r \geq L_D$. The second integral is zero because the velocities $v(\rho)$ and $v(\rho + r)$ are always uncorrelated ($\rho \leq L_D$ and $\rho + r \geq L_D$). Thus:

$$R_E^{(sim)}(r) = \frac{1}{L_D}\int_0^{L_D - r} \hat{R}_E(\rho)\, \mathrm{d}\rho = \left(1 - \frac{r}{L_D}\right)\hat{R}_E(r). \tag{25}$$

The corresponding simulated integral lengthscale is:

$$\begin{aligned} L_E^{(sim)} &= \int_0^{\infty} R_{E(sim)}(r)\, \mathrm{d}r = \int_0^{L_D}\left(1 - \frac{r}{L_D}\right)R_E(r)\, \mathrm{d}r \\ &= L_{E(\parallel)}\left\{1 - \frac{L_{E(\parallel)}}{L_D}\left[1 - \exp\left(-\frac{L_D}{L_{E(\parallel)}}\right)\right]\right\}; \end{aligned} \tag{26}$$

the last equality holds for $R_E(r)$ given by (22). This result shows that the introduction of a cutoff length reduces the integral lengthscale that is actually simulated: if we take $L_D = L_{E(\|)}$, then $L_E^{(sim)} = L_{E(\|)}/e = L_E/e$. Results of numerical simulations of the correlation $R_E^{(sim)}(r)$, presented in Fig. 4, confirm predictions of the theoretical analysis, as given by (25) with (21). In plot 4a, the exponential correlation coefficient $R_E(r)$, Eq. (22), is used for the Eulerian step with no cutoff length, whereas in plot 4b a finite cutoff length is introduced. Plot 4c with $R_E(r) = 1$ corresponds to the ELT method.

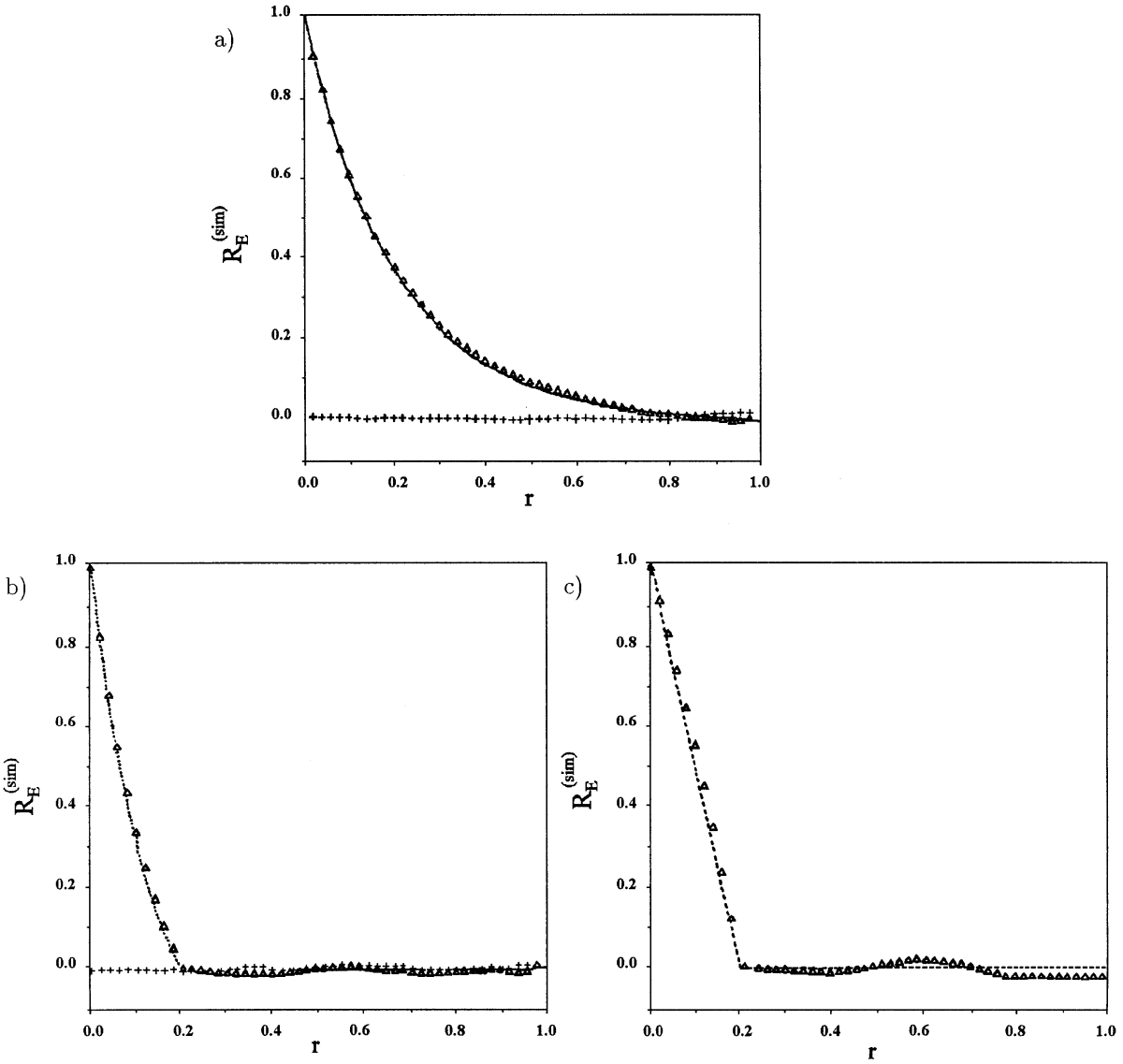

Fig. 4. Numerical realisation of the spatial correlation coefficient: (a) with continuous velocity sequence ($L_D = \infty$); (b) exponential correlation (22) with a finite cutoff length $L_D = 0.2$; (c) constant correlation with a finite cutoff length $L_D = 0.2$. Lines—theoretical curves, symbols (triangles)—simulation.

It is thus clear that methods with a finite cutoff length, where the accompanying fluid particle is changed every several time steps, are inconsistent. The artificial decrease of the velocity correlation is due to the introduction of a finite value of L_D. Moreover, in the simulations with $L_D = \infty$, the use of (21) would be unacceptable, for the same fluid particle would be followed all the time, whatever the distance r. Consequently, it seems preferable to change the driving fluid particle attached to the solid one at each time step.

3.3. Turbulent kinetic energy of the fluid 'seen' by the particles

As already precised, the formula for the Eulerian step is proposed by analogy with the Lagrangian one. Therefore, the coefficients a_E and b_E in Eq. (15) are calculated from the conditions that the averaged spatial correlation $R_E(r)$ be respected and the kinetic energy of the fluid 'seen' be conserved. However, unlike the Lagrangian correlation coefficient a_L, the Eulerian one, a_E, is calculated separately for each fluid-solid particle pair from the distance between them and, consequently, is not constant. In order to see the practical implications of this fact, we take the ensemble mean of (15) squared:

$$\begin{aligned}\langle (v^{n+1})^2\rangle &= \langle (a_E v_L + b_E e)^2\rangle = \left\langle \left[\exp\left(-\frac{r}{L_E}\right) v_L \right]^2 \right\rangle + \langle b_E^2 e^2\rangle + \left\langle 2\exp\left(-\frac{r}{L_E}\right) v_L e \right\rangle \\ &= \left\langle \exp\left(-\frac{2r}{L_E}\right) v_L^2 \right\rangle + \left\langle 1 - \exp\left(-\frac{2r}{L_E}\right) \right\rangle \sigma_f^2.\end{aligned} \tag{27}$$

If we accept the equality

$$\left\langle \exp\left(-\frac{2r}{L_E}\right) v_L^2 \right\rangle = \left\langle \exp\left(-\frac{2r}{L_E}\right) \right\rangle \langle v_L^2\rangle = \left\langle \exp\left(-\frac{2r}{L_E}\right) \right\rangle \sigma_f^2, \tag{28}$$

we find $\langle (v^{n+1})^2\rangle = \sigma_f^2$, i.e. the fluid turbulent energy is conserved. In fact, for (28) to hold, r and v_L should be uncorrelated—which is obviously not the case, because of (13) and (17). Let us try to quantify the influence of this correlation on the kinetic energy of the fluid 'seen' during a numerical simulation. We call σ_n the value of $\sqrt{\langle (v^n)^2\rangle}$. If the fluid turbulent energy were conserved in the simulation, we would have $\sigma_n = \sigma_f$ for any n. Let us compute σ_{n+1} from (27), for $r \ll L_E$:

$$\begin{aligned}\sigma_{n+1}^2 &\approx \left\langle \left(1 - \frac{2r}{L_E}\right) (a_L v^n + b_L e^n)^2 \right\rangle + \frac{2}{L_E} \langle r\rangle \sigma_f^2 \\ &\approx \left\langle \left(1 - \frac{2r}{L_E}\right) a_L^2 (v^n)^2 \right\rangle + \left\langle 1 - \frac{2r}{L_E} \right\rangle (1 - a_L^2)\sigma_f^2 + \frac{2}{L_E} \langle r\rangle \sigma_f^2;\end{aligned} \tag{29}$$

r stands for the instantaneous relative distance and is given by $r = |v^n - v_p^n|\,\Delta t$. Consider first the case of small particles which closely follow fluid motion (recalling that here $g = 0$). In the limit $\tau_p \to 0$ we have $v_r^n = v_p^n - v^n \to 0$, hence $\langle v_r^n\rangle \to 0$ and

$$\langle (v_{\mathrm{r}}^n)^2 \rangle = \sigma_{\mathrm{f}}^2 \frac{1}{1 + T_{\mathrm{L}}/\tau_{\mathrm{p}}} \to 0. \tag{30}$$

Using the formulae for the moments of the random variable $|v^n|$ where $v^n \in \mathcal{N}(0,\sigma_n)$ (Papoulis, 1991)

$$\langle |v^n| \rangle = \sqrt{\frac{2}{\pi}}\sigma_n, \quad \langle |v^n|^3 \rangle = 2\sqrt{\frac{2}{\pi}}\sigma_n^3, \tag{31}$$

for $r \to 0$ we obtain

$$\langle r \rangle = \langle |v_{\mathrm{r}}^n| \rangle \Delta t = \sqrt{\frac{2}{\pi}} \Delta t \sqrt{\langle (v_{\mathrm{r}}^n)^2 \rangle} \to 0 \tag{32}$$

and $\langle r^2 \rangle = \langle (v_{\mathrm{r}}^n)^2 \rangle \to 0$. In the other limit of large particles:

$$v_{\mathrm{p}}^n \approx 0 \quad \Rightarrow \quad r \approx |v^n| \Delta t. \tag{33}$$

Using this, we write (29) in the form

$$\begin{aligned} \sigma_{n+1}^2 &\approx a_{\mathrm{L}}^2 \sigma_n^2 - a_{\mathrm{L}}^2 \frac{2\Delta t}{L_{\mathrm{E}}} \langle |v^n|^3 \rangle + (1 - a_{\mathrm{L}}^2)\sigma_{\mathrm{f}}^2 + a_{\mathrm{L}}^2 \frac{2\Delta t}{L_{\mathrm{E}}} \langle |v^n| \rangle \sigma_{\mathrm{f}}^2 \\ &= \sigma_{\mathrm{f}}^2 + a_{\mathrm{L}}^2 (\sigma_n^2 - \sigma_{\mathrm{f}}^2) + \frac{2\Delta t}{L_{\mathrm{E}}} a_{\mathrm{L}}^2 \sqrt{\frac{2}{\pi}} \sigma_n (\sigma_{\mathrm{f}}^2 - 2\sigma_n^2). \end{aligned} \tag{34}$$

We notice that for $\sigma_n = \sigma_{\mathrm{f}}$ one has $\sigma_{n+1} < \sigma_n$. On the other hand, direct inspection of (34) shows that there exists a stationary value of the turbulent kinetic energy of the fluid 'seen'. In other words, there exists σ_n such that $0 < \sigma_n < \sigma_{\mathrm{f}}$ and $\sigma_{n+1} = \sigma_n$. We suppose that a qualitatively similar behaviour is typical for any particle size. Indeed, the numerical realization of the method confirms that the turbulent kinetic energy of the fluid 'seen', calculated as the ensemble mean $\langle (v_n)^2 \rangle$, decreases from its initial value by a certain amount (depending on the particle diameter) and levels off after a time of the order of the particle relaxation time τ_{p}. Typical results for three particle diameters d are plotted in Fig. 5. This result shows an important drawback of the model, for the kinetic energy of the fluid 'seen' by the particles should not depend on the particle diameter.

3.4. Particle inertia effect

In this subsection, we still consider the no-gravity case; therefore, only particle inertia influences turbulent dispersion. In particular, large heavy particles hardly respond to the fluid motion and are nearly at a standstill; for such particles, the timescale of the fluid 'seen' T_{L}^* is approximately the Eulerian time scale T_{E}. Yet, due to the use of the instantaneous relative velocities which are not negligible here, the Lagrangian model we are considering does not meet this physical condition.

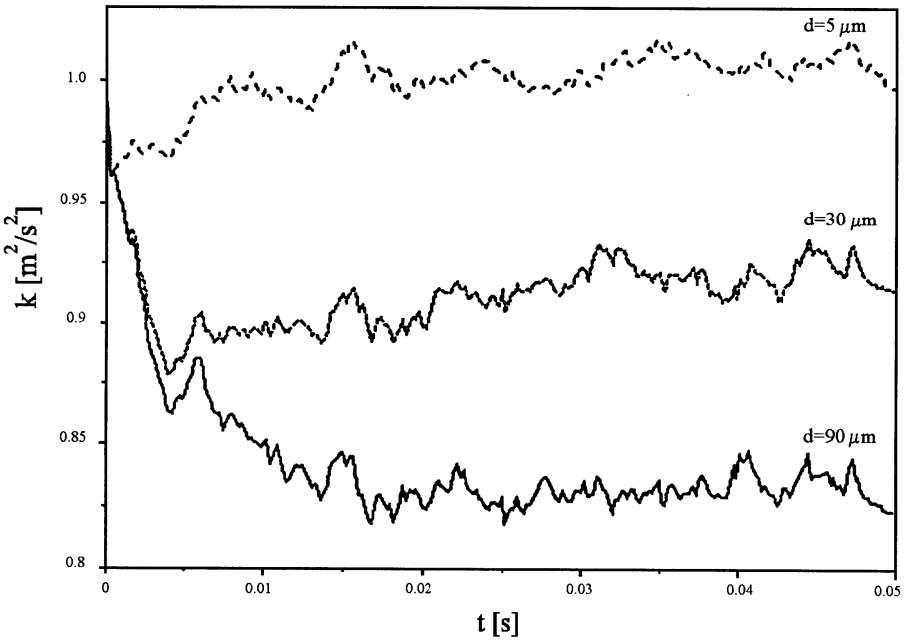

Fig. 5. Mean turbulent energy of the fluid 'seen'; simulation using Eqs. (13) and (15). $T_L = 0.0233$ s, $\tau_p(d = 5\ \mu\text{m}) = 2{\cdot}10^{-4}$ s, $\tau_p(d = 30\ \mu\text{m}) = 3{\cdot}10^{-3}$ s, $\tau_p(d = 90\ \mu\text{m}) = 5{\cdot}10^{-2}$ s.

To justify this statement, consider correlation of the fluid velocity along particle trajectories:

$$R_L^*(\Delta t) = \left\langle \exp\left(-\frac{r}{L_E}\right) \exp\left(-\frac{\Delta t}{T_L}\right)\right\rangle \approx \left\langle \exp\left[-\Delta t\left(\frac{1}{T_L} + \frac{|\mathbf{v}r|}{L_E}\right)\right]\right\rangle. \tag{35}$$

The relative velocity $\mathbf{v}_r$ is a random vector of zero mean; its components can be assumed to be independent Gaussian variables with a variance $\sigma_r^2 = \langle v_r^2 \rangle$ given by (30). Hence

$$\begin{aligned} \langle |\mathbf{v}_r| \rangle &= \frac{1}{(2\pi)^{3/2}\sigma_r^3} \int\int\int_{-\infty}^{\infty} \sqrt{v_{rx}^2 + v_{ry}^2 + v_{rz}^2}\, \exp\left(-\frac{v_{rx}^2 + v_{ry}^2 + v_{rz}^2}{2\sigma_r^2}\right) \mathrm{d}v_{rx}\mathrm{d}v_{vy}\mathrm{d}v_{rz} \\ &= \frac{8\pi}{(2\pi)^{3/2}}\sigma_r = C\sigma_r = C\frac{\sigma_f}{\sqrt{1 + T_L/\tau_p}} \end{aligned} \tag{36}$$

and

$$R_L^*(\Delta t) = \exp\left[-\Delta t\left(\frac{1}{T_L} + \frac{C}{T_E\sqrt{1 + T_L/\tau_p}}\right)\right]. \tag{37}$$

As a consequence, the resulting integral timescale of the fluid 'seen', $T_L^* = \int_0^\infty R_L^*(t)\ \mathrm{d}t$, is equal to

$$T_{\mathrm{L}}^{*} = T_{\mathrm{L}}\left(1 + \frac{\beta C}{\sqrt{1 + T_{\mathrm{L}}/\tau_{\mathrm{p}}}}\right)^{-1} \tag{38}$$

where $C = 2\sqrt{2\pi}$ and $\beta = T_{\mathrm{L}}/T_{\mathrm{E}}$. The velocity correlation of the fluid seen by nearly immobile heavy particles should be close to the Eulerian temporal correlation:

$$R_{\mathrm{L}}^{*}(\Delta t) \approx \exp\left(-\frac{\Delta t}{T_{\mathrm{E}}}\right). \tag{39}$$

However, even in the absence of gravity, the LIV model involves a significant decrease of T_{L}^{*} that does not tend towards the correct limit (the Eulerian scale T_{E}) for large particles, $\tau_{\mathrm{p}}/T_{\mathrm{L}} \gg 1$. The resulting time scale is equal to $T_{\mathrm{L}}^{*} = T_{\mathrm{L}}/(1 + \beta C) \approx 0.4\, T_{\mathrm{L}}$.

This short analysis states clearly that in the case of large heavy particles the correlation $R_{\mathrm{L}}^{*}(t)$, the timescale of the fluid 'seen', T_{L}^{*}, and consequently the particle diffusivity are artificially reduced by the very principle of the method considered. The asymptotic case that we have just considered reveals a serious discrepancy (the timescale is reduced more than twice). Similar trends are visible for smaller particles. In order to demonstrate and quantify this discrepancy, numerical simulations using (13) and (15) have been performed for two particle diameters: 5 and 57 μm, the same as in the Wells and Stock (1983) experiment. Gravity is still switched off and thus there is no mean drift. In this case, the timescales of the fluid 'seen' are always greater than T_{L}. If we consider that the increase which has been found for a certain range of particle diameters is due to instantaneous turbulent structures that cannot be taken into account within the framework of statistical Lagrangian model, then the different timescale values are between T_{L} and T_{E}. Therefore, since $T_{\mathrm{L}} \approx T_{\mathrm{E}}$ ($T_{\mathrm{L}} = 0.92\, T_{\mathrm{E}}$), the timescale T_{L}^{*} for any particle inertia should be greater than T_{L} in the absence of external forces.

It is evident from Fig. 6 that the LIV model does not respect this physical condition. The effect is not clearly marked for the 5 μm particle since the relative velocities remain small. On the contrary, in the case of 57 μm particles, the relative velocities are larger due to higher particle inertia and bring about a significant decrease of the timescale T_{L}^{*}.

Finally, in Table 1 we present the results of the numerical simulation of particle dispersion in stationary isotropic turbulence using the LIV model. Mean-square displacement values, $S_{\mathrm{p}}(t) = \langle X_{\mathrm{p}}^{2}(t) \rangle$, for two particle diameters are compared to the classical Taylor formula (c.f. Hinze, 1975). As before, results are not satisfactory; however, for smaller particles, S_{p} values remain closer to fluid diffusion.

Table 1
Particle dispersion in stationary isotropic turbulence. $T_{\mathrm{L}} = 0.2$ s, $\sigma_{\mathrm{f}} = 1.0$ m/s, $\rho_{\mathrm{p}} = 2400$ kg/m^3, $\rho_{\mathrm{f}} = 1.17$ kg/m^3

	$S_{\mathrm{p}}(T_{\mathrm{L}})$	$S_{\mathrm{p}}(5T_{\mathrm{L}})$
Theory (Taylor)	0.020	0.214
$d = 5$ μm	0.018	0.185
$d = 57$ μm	0.013	0.136

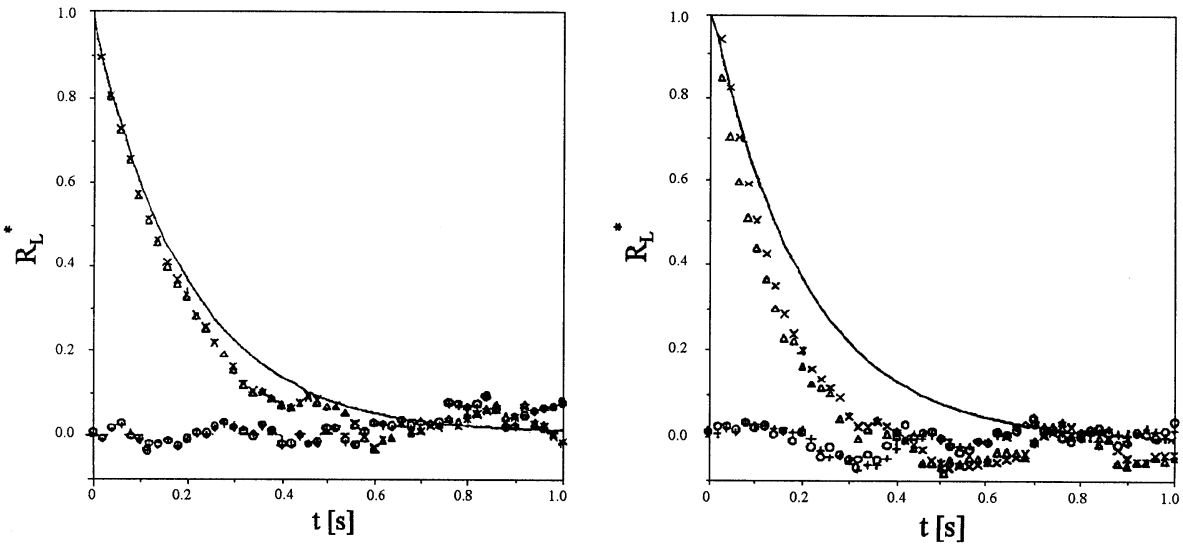

Fig. 6. Velocity correlation coefficient $R_L^*(t)$ for the fluid seen by particles: (a) $d = 5\ \mu$m; (b) $d = 57\ \mu$m. Simulation using LIV model [Eqs. (13) and (15)]. Solid line—exponential correlation exp $(-t/T_L)$; × and △—two typical simulations of the correlation for the same velocity component; + and *o*—the cross-correlation (zero in isotropic turbulence; the statistical noise level is clearly seen).

3.5. Effect of crossing trajectories

When gravity is introduced in the picture, a mean drift triggers the crossing trajectory effect. In this case, the erroneous trends displayed in the previous section still lead to an incorrect behaviour of the model based on the instantaneous relative velocity. This is due to the fact that the mean free-fall velocity of particles in a turbulent fluid, $v_g = |\langle \mathbf{v}_p \rangle| = \tau_p\, g$ is 'screened' by the ensemble mean relative velocity, calculated as $v_r = \langle |\mathbf{v}_p - \mathbf{v}| \rangle$. Results of numerical simulation confirm that for the small particles we have $v_g \ll v_r$. As a consequence, the timescales predicted by the LIV model are considerably reduced compared to those obtained from the analysis of Csanady. The discrepancies are a bit less marked for the large particles when gravity is acting on them.

4. New Particle Dispersion Model

Conclusions from a thorough analysis of the LIV model, backed by numerical simulations, will now serve to advance new propositions. Particular emphasis will be put on the Eulerian step which proves to be the most difficult to cope with in order to obtain better modelling of both particle inertia and crossing trajectory effects. Our propositions are developed from a different starting point than in the LIV model. Namely, we consider an ensemble of fluid (or solid) particles having some average properties, instead of an individual particle and we consequently adopt this point of view. It should be added here that a similar 'philosophy' is

already inherent to the Lagrangian step since the correlation coefficient used is representative of the average Lagrangian particle behaviour. A new model, based on the above-presented approach, will be proposed in the sequel.

4.1. Inertia effect

First, consider the no-gravity case. In the limit of large, nearly immobile heavy particles $\sigma_p/\sigma_f \to 0$) the timescale 'seen' is T_E whereas T_L is the correct value for the other limit of extremely small particles which behave nearly as fluid elements.

To take account of particle inertia effect, let us consider a schematic drawing (Fig. 7) where one possible realization of the turbulent velocity field is plotted as an example. The average distance covered by the fluid particle during the time interval Δt is $O(\sigma_f \Delta t)$ since $\langle |v| \rangle = \sigma_f \sqrt{2/\pi} = O(\sigma_f)$. To calculate the velocity $\mathbf{v}^{n+1}$ of the fluid seen by the particle at the point P^{n+1}, we make use of two velocities at the time t^{n+1} correlated with $\mathbf{v}^n$ and obtained from the Langevin equation model:

$$\mathbf{v}_L = a_L \mathbf{v}^n + b_L \mathbf{e}_L, \quad \mathbf{v}_E = a_E \mathbf{v}^n + b_E \mathbf{e}_E \tag{40}$$

with

$$\begin{aligned} a_L &= \exp\left(-\frac{\Delta t}{T_L}\right), \quad b_L = \sigma_f \sqrt{1 - a_L^2}, \quad \mathbf{e}_L \in \mathcal{N}(0, 1), \\ a_E &= \exp\left(-\frac{\Delta t}{T_E}\right), \quad b_E = \sigma_f \sqrt{1 - a_E^2}, \quad \mathbf{e}_E \in \mathcal{N}(0, 1). \end{aligned} \tag{41}$$

For the fluid velocity 'seen' by the particle, we propose the following formula:

$$\mathbf{v}^{n+1} = a_1 \mathbf{v}_L + a_2 \mathbf{v}_E + b\mathbf{e}. \tag{42}$$

The physical reasoning behind this expression is that the average position of the solid particle P^{n+1} is between F^n and F^{n+1}, with the distance $P^n P^{n+1} = O(\sigma_p \Delta t)$. If the particle were

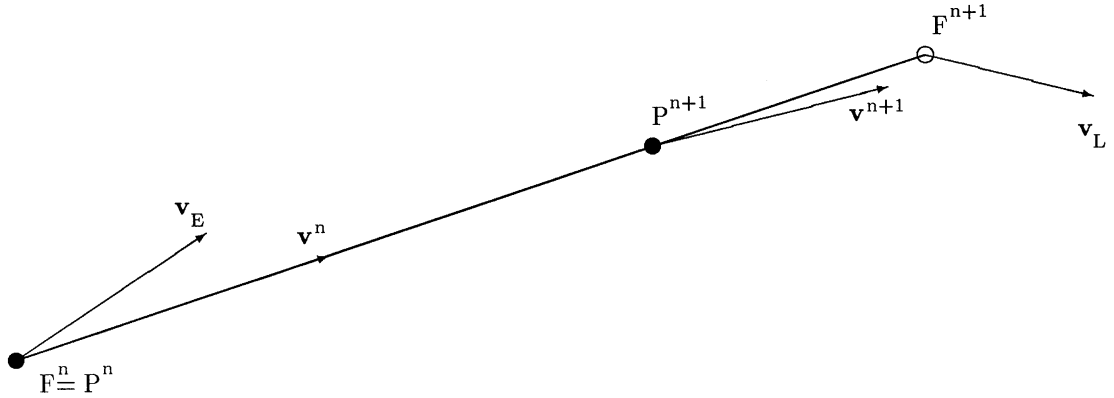

Fig. 7. Fluid velocity vectors at t^n (vector $\mathbf{v}^n$) and at t^{n+1} (vectors $\mathbf{v}^{n+1}$, $\mathbf{v}_L$, $\mathbf{v}_E$).

certain to be at P^{n+1}, we would omit the third, random term on the r.h.s. of (42), so that it would be simply an interpolation formula in a given deterministic velocity field at t^{n+1}. However, this is not the case; the pdf contour lines of the particle position P^{n+1} in homogeneous turbulence, given a fluid velocity $\mathbf{v}^n$ at P^n, are schematically represented in Fig. 8.

A large particle (case a) is nearly certain to stay close to its previous location $P^n = F^n$, whereas a small one (case c) is found in the vicinity of the twin fluid particle position F^{n+1}. For a medium-size particle (case b), the pdf of its position is more 'blurred'. Actually, in this case the random term in (42) will be much more significant (as we will see soon) that in the other two cases. Thus, (42) can be regarded as a spatial interpolation formula with some uncertainty added which depends on the correlation level of fluid and solid particle motion.

To find the coefficients a_1, a_2 and b in (42), we require that given velocity correlations be respected:

$$\langle v_{\mathrm{L}} v_{\mathrm{E}} \rangle = \sigma_{\mathrm{f}}^2 \exp\left(-\frac{\sigma_{\mathrm{f}} \Delta t}{L} \right) = \sigma_{\mathrm{f}}^2 \exp\left(-\frac{\Delta t}{T_{\mathrm{E}}} \right), \tag{43}$$

$$\langle v^{n+1} v_{\mathrm{E}} \rangle = \sigma_{\mathrm{f}}^2 \exp\left(-\frac{\sigma_{\mathrm{p}} \Delta t}{L} \right) = \sigma_{\mathrm{f}}^2 \exp\left(-x \frac{\Delta t}{T_{\mathrm{E}}} \right), \tag{44}$$

$$\langle v^{n+1} v_{\mathrm{L}} \rangle = \sigma_{\mathrm{f}}^2 \exp\left(-\frac{(\sigma_{\mathrm{f}} - \sigma_{\mathrm{p}}) \Delta t}{L} \right) = \sigma_{\mathrm{f}}^2 \exp\left(-(1-x) \frac{\Delta t}{T_{\mathrm{E}}} \right). \tag{45}$$

We multiply (42) by v_{L}, v_{E}, v_{n+1}, respectively, take the ensemble mean and substitute for the velocity correlations. We thus obtain a system of three equations for a_1, a_2, b that yields:

$$a_1 = \frac{a^{1-x} - a^{1+x}}{1 - a^2}, \quad a_2 = \frac{a^x - a^{2-x}}{1 - a^2}, \quad b^2 = \sigma_{\mathrm{f}}^2 (1 - a_1^2 - a_2^2 - 2 a_1 a_2) \tag{46}$$

with

$$x = \frac{\sigma_{\mathrm{p}}}{\sigma_{\mathrm{f}}}, \quad a = \exp\left(-\frac{\Delta t}{T_{\mathrm{E}}} \right). \tag{47}$$

Now, the correlations between two successive fluid velocities 'seen' can be written as:

$$\langle v^{n+1} v^n \rangle = a_1 \langle v_{\mathrm{L}} v^n \rangle + a_2 \langle v_{\mathrm{E}} v^n \rangle = \sigma_{\mathrm{f}}^2 (a_1 a_{\mathrm{L}} + a_2 a_{\mathrm{E}}). \tag{48}$$

Using the expressions for the coefficients and considering small time steps $\Delta t \ll T_{\mathrm{L}}$, we develop (48) into a Taylor series. The final result writes

$$\frac{1}{\sigma_{\mathrm{f}}^2} \langle v^{n+1} v^n \rangle \approx 1 - \Delta t \left(\frac{x}{T_{\mathrm{L}}} + \frac{1-x}{T_{\mathrm{E}}} \right) \approx \exp\left(-\frac{\Delta t}{T_{\mathrm{L}}^*} \right), \tag{49}$$

where T_{L}^* is defined as:

$$\frac{1}{T_{\mathrm{L}}^{*}}=\frac{x}{T_{\mathrm{L}}}+\frac{1-x}{T_{\mathrm{E}}}. \tag{50}$$

The form of the expression (46) for b assures that in the two limits, $x = 0$, $x = 1$, a random term in (42) is equal to zero; b attains a maximum for some intermediate value of x (for $T_{\mathrm{L}}\approx T_{\mathrm{E}}$, $x \approx 0.5$) which agrees with Fig. 8.

Eq. (50) can also be thought of as an alternative to the reasoning presented above. Namely, this equation may be proposed from the outset as an interpolation formula for T_{L}^{*} to satisfy the two limits: $T_{\mathrm{L}}^{*} = T_{\mathrm{L}}$ for $\tau_{\mathrm{p}}\to 0$ and $T_{\mathrm{L}}^{*} = T_{\mathrm{E}}$ for $\tau_{\mathrm{p}}\to\infty$. The interpolation is based on $x = \sigma_{\mathrm{p}}/\sigma_{\mathrm{f}}$, the ratio of particle to fluid r.m.s. turbulent velocity. Actually, the physical underlying parameter is τ_{p}, the particle characteristic time. However, τ_{p} spans the whole real axis, whereas x is a bounded variable. Both are closely related by the Tchen's expression (3) confirmed by LES: $\tau_{\mathrm{p}} = T_{\mathrm{L}}(1-x^{2})/x^{2}$.

4.2. Mean drift effect—first proposal (LMV)

The first idea that comes to mind in order to improve the Eulerian step (15) consists in taking the relative distance between the solid and the fluid particle, calculated on the basis of the mean relative velocity:

$$r = |\langle \mathbf{v}_{\mathrm{p}}^{n}\rangle - \langle \mathbf{v}^{n}\rangle|\Delta t \tag{51}$$

instead of previously used expression

$$r = |\mathbf{v}_{\mathrm{p}}^{n} - \mathbf{v}^{n}|\Delta t. \tag{52}$$

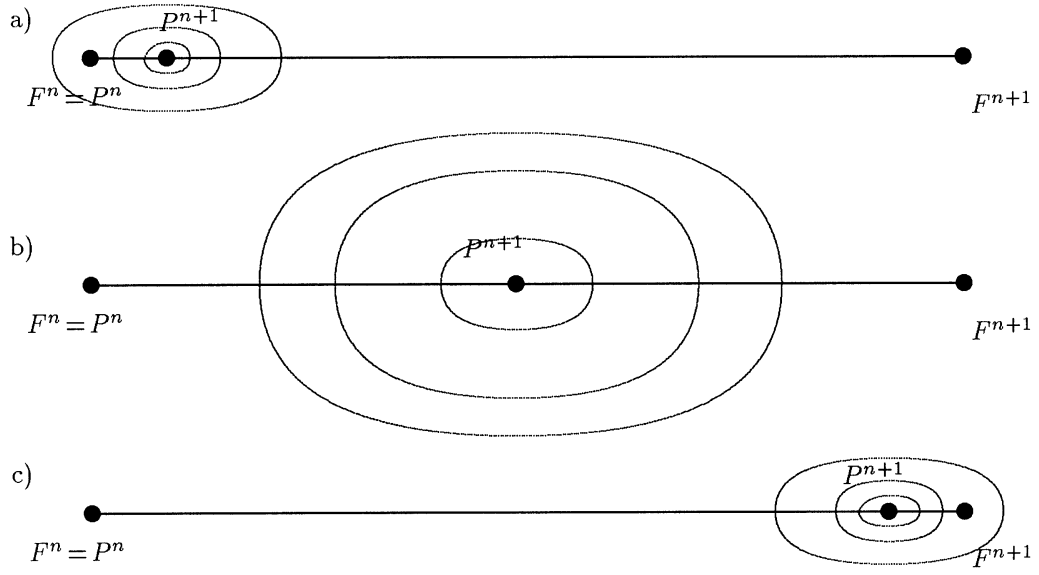

Fig. 8. The pdf contours of particle position for three different inertia parameters.

For the case of stationary isotropic turbulence in the gravity field, we have $\langle \mathbf{v}^n \rangle = 0$ and $\mathbf{v}_g = \langle \mathbf{v}_p^n \rangle$. In these expressions, $\mathbf{v}^n$ stands for the fluid velocity 'seen' and $\mathbf{v}_g$ is the ensemble mean particle free-fall velocity (the average settling velocity). In practical simulations, the ensemble mean calculated at the previous time step is taken as the current value.

In (50), no-gravity case is considered ($\xi = 0$). When gravity is non-zero, its influence is taken into account via the mean slip velocity. The model with gravity is schematically illustrated in Fig. 9. The average location of the solid particle is P^{n+1}, while P_0^{n+1} is its location with no gravity. The first simulation step consists in using the interpolation formula [symbols as in Eq. (42)]

$$\mathbf{v}_0^{n+1} = a_1 \mathbf{v}_L + a_2 \mathbf{v}_E + b\mathbf{e} \tag{53}$$

and in the second step the Eulerian spatial correlation is used

$$\mathbf{v}^{n+1} = a_S \mathbf{v}_0^{n+1} + b_S \mathbf{e}_S \tag{54}$$

with

$$a_S = \exp\left(-\frac{|\mathbf{v}_g \Delta t|}{L_E} \right), \quad b_S = \sigma_f \sqrt{1 - a^2}, \quad \mathbf{e}_S \in \mathcal{N}(0, 1), \tag{55}$$

where L_E corresponds to $L_{E(\|)}$ in the direction parallel to the gravity and to $L_{E(\perp)}$ in two other (perpendicular) directions. This first proposal, consisting of Eqs. (40), (53) and (54), will temporarily be called the Langevin model with mean relative velocity (LMV).

Compute now the correlation of two subsequent fluid velocities along the particle trajectory. Using (54), substituting for $\mathbf{v}_L$ from (40) and taking the ensemble mean, we obtain:

$$\langle v_i^n v_i^{n+1} \rangle = \sigma_f^2 \exp\left[-\Delta t \left(\frac{1}{T_L^*} + \frac{|\mathbf{v}_g|}{L_E} \right) \right]. \tag{56}$$

Let us introduce two new variables $T_{L(\|)}^*$ and $T_{L(\perp)}^*$, defined by:

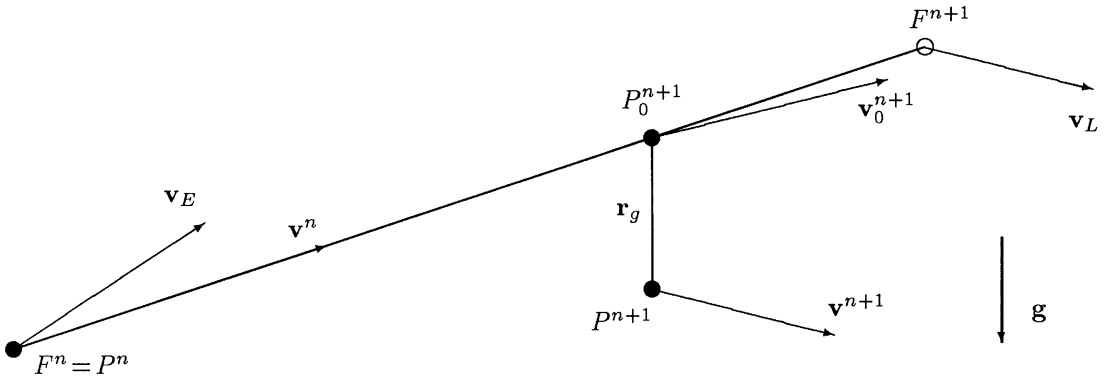

Fig. 9. Velocities of fluid particles—schematic drawing. Vector $\mathbf{v}^n(t^n)$ and vectors $\mathbf{v}^{n+1}$, $\mathbf{v}_L$, $\mathbf{v}_E$ at t^{n+1}.

$$\frac{1}{T^*_{\mathrm{L}(\|)}} = \frac{1}{T^*_{\mathrm{L}}} + \frac{|\mathbf{v}_{\mathrm{g}}|}{\sigma_{\mathrm{f}} T_{\mathrm{E}}}, \quad \frac{1}{T^*_{\mathrm{L}(\perp)}} = \frac{1}{T^*_{\mathrm{L}}} + \frac{2|\mathbf{v}_{\mathrm{g}}|}{\sigma_{\mathrm{f}} T_{\mathrm{E}}}. \tag{57}$$

We also define $\beta^* = T_{\mathrm{L}}^*/T_{\mathrm{E}} = \sigma_{\mathrm{f}} T_{\mathrm{L}}^*/L_{\mathrm{E}}$ and $\xi = |\mathbf{v}_{\mathrm{g}}|/\sigma_{\mathrm{f}}$ (nondimensional settling velocity). This implies that the Lagrangian step and the Eulerian step with the mean relative distance can be melted into a single expression which represents, in fact, a Langevin model (11) with $T_{\mathrm{L}}^*(\xi)$ equal to:

$$T^*_{\mathrm{L}(\|)}(\xi) = \frac{T^*_{\mathrm{L}}}{1 + \xi\beta^*}, \quad T^*_{\mathrm{L}(\perp)}(\xi) = \frac{T^*_{\mathrm{L}}}{1 + 2\xi\beta^*}, \tag{58}$$

where T_{L}^* given by (50). As opposed to the Langevin model with instantaneous relative velocity (LIV) there is no pitfall since $\mathbf{v}_{\mathrm{g}}$ is a constant. Also, the proposed Eulerian step formula (54), contrary to the previous one, Eq. (15), gives an acceptable behaviour of dense particles in the limit $\xi = 0$. In other words, in the absence of an external force field, this model gives for the integral timescale of the fluid 'seen', T_{L}^*:

$$T^*_{\mathrm{L}(|)}(\xi = 0) = T^*_{\mathrm{L}(\perp)}(\xi = 0) = T^*_{\mathrm{L}}. \tag{59}$$

4.3. Mean drift effect—final proposal (LMC)

Although the LMV model is correctly constructed as far as the kinetic energy of the fluid seen by the particles and the inertia effect are concerned, simulation results of the crossing trajectory effect using (58) in the case of stationary isotropic turbulence do not give full satisfaction. Namely, as compared to the LES data (Deutsch, 1992), both $T_{\mathrm{L}(\|)}^*(\xi)$ and $T_{\mathrm{L}(\perp)}^*(\xi)$ diminish too quickly as ξ increases. This may be explained by the fact of having applied the two-step approach, i.e. finding $v_0^{n+1} = v(\xi = 0)$ first and then $v^{n+1} = v(\xi)$ based on this value, which is supposed to somehow introduce an artificial decorrelation. This is why we propose a modification to simulate the particle dispersion in an external force (gravity) field. In the limit $\mathbf{v}_{\mathrm{g}} \to 0$, it will boil down to the previous one. Let us consider once again a schematic drawing, Fig. 9. As before, F^n and P^n represent the fluid element and the particle position at $t = t^n$, respectively. Let us take

$$\sigma_{\mathrm{p}(\|)} = \sqrt{\langle v^2_{\mathrm{p}(\|)} \rangle}, \quad \sigma_{\mathrm{p}(\perp)} = \sqrt{\langle v^2_{\mathrm{p}(\perp)} \rangle},$$

which stand for the r.m.s. particle fluctuating velocities in the directions parallel and perpendicular to $\mathbf{g}$, respectively. The mean distance travelled by the fluid particle in the time interval Δt is $R_{\mathrm{F}} = |\mathbf{R}_{\mathrm{F}}| = |F^n F^{n+1}| = O(\sigma_{\mathrm{f}} \Delta t)$. The mean distance travelled by its virtual twin dense particle P_0, i.e. the particle situated at t^n at the same point as the fluid element ($F^n = P^n$), belongs to the range $\sigma_{\mathrm{p}(\perp)} \le \sigma_{\mathrm{p}} \le \sigma_{\mathrm{p}(\|)}$, depending on the direction of the vector $F^n F^{n+1}$ with respect to gravity. By definition, there is no influence of $\mathbf{g}$ on the motion of P_0.

We assume that the virtual particle position P_0^{n+1} lies on the surface of an ellipsoid centered on F^n, whose axes are equal to $\sigma_{\mathrm{p}(\|)}$ in the direction of gravity and to $\sigma_{\mathrm{p}(\perp)}$ in the two other directions (Fig. 10). Then we suppose that the 'true' particle position P^{n+1} is determined by P_0^{n+1}, with $r_{\mathrm{g}} = |P_0^n P_0^{n+1}| = |\mathbf{v}_{\mathrm{g}}| \Delta t$. As before, the displacement r_{g} represents the effect of the

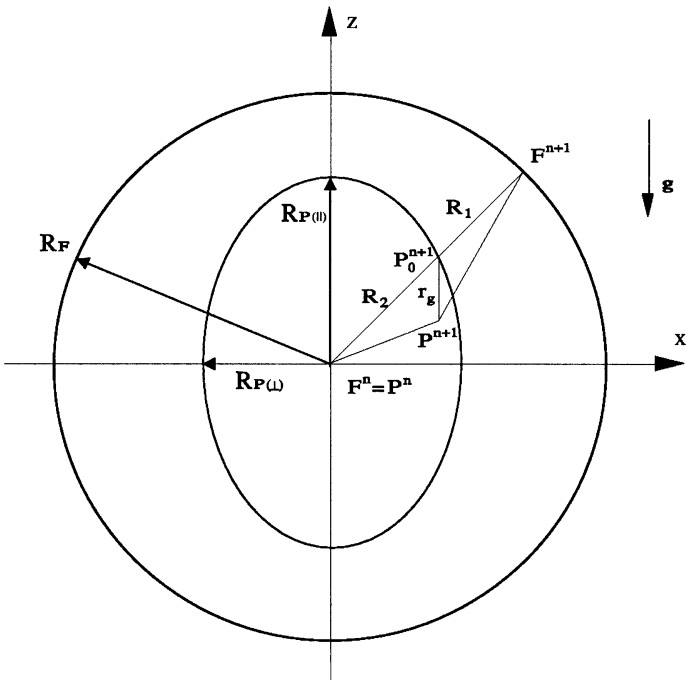

Fig. 10. The ellipsoid of particle displacements.

gravity field. The new approach consists in calculating the fluid velocity $\mathbf{v}^{n+1}$ 'seen', i.e. at the point P^{n+1}, from two velocities at $t = t^{n+1}$: $\mathbf{v}_L$ at the point F^{n+1}, respecting the Lagrangian correlation with $\mathbf{v}^n$, and $\mathbf{v}_E$ at the point F^n, satisfying the Eulerian temporal correlation with $\mathbf{v}^n$. We simulate $\mathbf{v}_L$ and $\mathbf{v}_E$ using the Langevin equation in the discrete form, Eqs. (40) and (41).

Let us come back to Fig. 9. Keeping in mind the fact that P_0^{n+1} is situated somewhere on the surface of the ellipsoid, we should consider Fig. 9 as one of possible realizations of the fluctuating velocity field at the mean fluid and solid particle locations. The idea of the model is to propose a Langevin-like equation to compute $\mathbf{v}^{n+1}$ from $\mathbf{v}_L$ and $\mathbf{v}_E$ [see Eq. (40)]:

$$v_i^{n+1} = a_{1i} v_{Li} + a_{2i} v_{Ei} + b e_i, \tag{60}$$

where a_{1i}, a_{2i} ($i = 1, 2, 3$) represent the weights, calculated from the mean spatial correlation coefficients. The latter are found as averages over all possible directions of particle displacements with regard to the direction of gravity; their meaning will become clear soon. This formula differs significantly from (42) proposed for the LMV model where weight coefficients were determined from correlations (43)–(45); now, the coefficients take also the non-zero slip velocity into account. For the case with no external force, Eq. (60) becomes identical with (42). On the other hand, with external force (gravity) present, (60) allows to compute v_i^{n+1} directly, contrary to the previously proposed two-step approach, (53) and (54). Actually, the above Eq. (60) is the keystone of the new model, called for brevity the Langevin

model with mean coefficients (LMC). The values of a_{1i}, a_{2i} depend on whether the respective velocity component is parallel or perpendicular to the gravity direction. In our notation (cf. Fig. 10) we define $a_{1(\parallel)}$, $a_{1(\perp)}$ so that $a_{11} = a_{12} = a_{1(\perp)}$ and $a_{13} = a_{1(\parallel)}$. In the same way $a_{2(\parallel)}$ and $a_{2(\perp)}$ are introduced. So, we rewrite (60) in the form

$$v_i^{n+1} = \begin{cases} a_{1(\perp)} v_{\mathrm{L}i} + a_{2(\perp)} v_{\mathrm{E}i} + b_{(\perp)} e_i & \text{for} \quad \mathrm{i} = 1,2 \\ a_{1(\parallel)} v_{\mathrm{L}i} + a_{2(\parallel)} v_{\mathrm{E}_i} + b_{(\parallel)} e_i & \text{for} \quad \mathrm{i} = 3. \end{cases} \tag{61}$$

To determine the unknown coefficients, first multiply (60) by v_{L} and take the ensemble mean. We obtain

$$\langle v^{n+1} v_{\mathrm{L}} \rangle = a_1 \langle v_{\mathrm{L}}^2 \rangle + a_2 \langle v_{\mathrm{E}} v_{\mathrm{L}} \rangle. \tag{62}$$

The same operation applied to (60) and v_{E} results in

$$\langle v^{n+1} v_{\mathrm{E}} \rangle = a_1 \langle v_{\mathrm{E}} v_{\mathrm{L}} \rangle + a_2 \langle v_{\mathrm{E}}^2 \rangle. \tag{63}$$

We introduce mean spatial correlation coefficients a_{LP}, a_{EP} and a_{EL} so that

$$a_{\mathrm{EL}} = \frac{\overline{\langle v_{\mathrm{E}} v_{\mathrm{L}} \rangle}}{\sigma_{\mathrm{f}}^2}, \quad a_{\mathrm{EP}} = \frac{\overline{\langle v_{\mathrm{E}} v^{n+1} \rangle}}{\sigma_{\mathrm{f}}^2}, \quad a_{\mathrm{LP}} = \frac{\overline{\langle v_{\mathrm{L}} v^{n+1} \rangle}}{\sigma_{\mathrm{f}}^2}. \tag{64}$$

An overbar has been added to stress the fact that all correlations should be considered as directional averages in space. We rewrite (62) and (63) as

$$a_{\mathrm{LP}} = a_1 + a_2 a_{\mathrm{EL}} \quad \text{and} \quad a_{\mathrm{EP}} = a_1 a_{\mathrm{EL}} + a_2 \tag{65}$$

which results in

$$a_1 = \frac{a_{\mathrm{EP}} a_{\mathrm{EL}} - a_{\mathrm{LP}}}{1 - a_{\mathrm{EL}}^2}, \quad a_2 = \frac{a_{\mathrm{LP}} a_{\mathrm{EL}} - a_{\mathrm{EP}}}{1 - a_{\mathrm{EL}}^2}. \tag{66}$$

Moreover, (61) yields

$$\sigma_{\mathrm{f}}^2 = \langle v^{n+1} v^{n+1} \rangle = a_1^2 \langle v_{\mathrm{L}}^2 \rangle + a_2^2 \langle v_{\mathrm{E}}^2 \rangle + 2 a_1 a_2 \langle v_{\mathrm{E}} v_{\mathrm{L}} \rangle + b^2. \tag{67}$$

Thus

$$b^2 = \sigma_{\mathrm{f}}^2 (1 - a_1^2 - a_2^2 - 2 a_1 a_2 a_{\mathrm{EL}}). \tag{68}$$

All the three velocity correlations in (64) can be determined from the following reasoning. Consider a spherical system of coordinates (r,θ,φ) centered at the point $F^n = P^n$. The formulae for our directionally averaged correlations write:

$$\begin{aligned}
\overline{\langle v_{\mathrm{E}i} v_{\mathrm{L}i}\rangle} &= \frac{1}{4\pi}\int_{\Omega}\langle v_{\mathrm{E}i}(0) v_{\mathrm{L}i}(R_{\mathrm{F}}\mathbf{r}^0)\rangle \mathrm{d}\Omega,\\
\overline{\langle v_{\mathrm{E}i} v_i^{n+1}\rangle} &= \frac{1}{4\pi}\int_{\Omega}\langle v_{\mathrm{E}i}(0) v_i^{n+1}(R_{\mathrm{P}}(\mathbf{r}^0)\mathbf{r}^0 - r_{\mathrm{g}}\mathbf{z}^0)\rangle \mathrm{d}\Omega,\\
\overline{\langle v_{\mathrm{L}i} v_i^{n+1}\rangle} &= \frac{1}{4\pi}\int_{\Omega}\langle v_{\mathrm{L}i}(R_{\mathrm{F}}\mathbf{r}^0) v_i^{n+1}(R_{\mathrm{P}}(\mathbf{r}^0)\mathbf{r}^0 - r_{\mathrm{g}}\mathbf{z}^0)\rangle \mathrm{d}\Omega,\\
& i = 1, 2, 3 \text{ (no sum over } i),
\end{aligned} \tag{69}$$

where $\mathrm{d}\Omega = \sin\theta\ \mathrm{d}\varphi\ \mathrm{d}\theta$ is the infinitesimal solid angle corresponding to vector $\mathbf{R}_{\mathrm{F}}$ (and the unit vector $\mathbf{r}^0$). In (69) use has been made of the fact that the pdf of the direction of $\mathbf{R}_{\mathrm{F}}$ is uniform. More technical details of the numerical procedure can be found elsewhere (Pozorski et al., 1993; Pozorski, 1995).

Summarizing this section: starting from (40), the first version of the new method (LMV) consists in a two-step scheme, (53) and (54), used to calculate the next velocity of the fluid element seen by a particle; its improvement (LMC model) proposes a new formula with use of only one expression (60) that contains both inertia and mean drift effects and relies on the averaging over all possible directions of fluid element displacement.

The principal idea of both above presented variants is to consider the dispersion process from the point of view of the 'mean' solid particle and the twin 'mean' fluid particle. In this process we implicitly skip one step in the averaging procedure. Namely, the complete reasoning that can be thought of should take into account all fluid particles by introduction of the pdf of their velocity. Instead, we make use of the fact that the velocity of the fluid particle is of the order of σ_{f}. Moreover, one should consider the probability density of the solid particle position, conditional on the twin fluid particle velocity. For further study, we suggest proceeding in this direction rather than to start the reasoning from the instantaneous solid particle position (and displacement) and to consider the accompanying fluid particle. This would allow to avoid the problems with ensemble averages of spatial correlation that might imply the non-conservation of the fluid turbulent kinetic energy during the simulation [cf. Eq. (29)].

Another point that deserves a comment concerns the relationship (if any) of the proposed method and the procedure originally put forward by Saffman (1963) to derive the Lagrangian correlation coefficient from the assumed form of the spatial and temporal Eulerian velocity spectra. Saffman's reasoning is based on the so-called Corrsin's conjecture, sometimes referred to as the independence approximation, which establishes a relation between Lagrangian and Eulerian correlation. However, the analogy is by no means complete: in the Corrsin hypothesis, an average is taken to calculate the Lagrangian correlation, while in our approach the procedure is still two-step and spatial averaging is applied to the Eulerian step only.

In our reasoning, we assumed that the particle displacement is of the order of $\sigma_{\mathrm{p}}\Delta t$ and thus avoided the integration [cf. Eq. (69)] over all space with a particular form of the pdf of displacement in a given direction. The fact that the pdf of the direction of displacement for the accompanying fluid particle is uniform allowed us to solve the problem of the particle (and the fluid 'seen') displacement by means of geometrical considerations in the spherical reference

system. Use has also been made of the axial symmetry of the problem (with regard to the direction of gravity). This somewhat heuristic procedure as well as the Langevin-type Eq. (60) are thought to be justified *a posteriori* by the obtained results on the simulation of turbulent dispersion.

5. Numerical Results on Particle Dispersion

This section presents the results of numerical simulations using new dispersion model (LMC) and the comparison with both experimental measurements and numerical data. The experiments are those of Snyder and Lumley (1971) and Wells and Stock (1983) for particle dispersion in grid turbulence. They are referred to as S&L and W&S, respectively. The 'numerical experiment' we refer to is the study of particle behaviour in a turbulent flow calculated from large eddy simulation (Deutsch, 1992). It has been argued that the numerical experiments can in some cases yield more detailed results than the experimental measurements. Therefore, comparison with these results constitutes a stringent test.

Below, we present results of the Lagrangian simulation of particle dispersion in grid turbulence and in isotropic stationary turbulence. In both cases, the numerical algorithm is essentially the same. Simulations consisted in tracking individual particle trajectories, released from a fixed point; particle dynamics is governed by (1) and (2). Velocity of the fluid seen that enters (1) was modelled by (40), (53) and (54) in the preliminary model (LMV), or by (40) and (60) in the final model (LMC). Usually, an ensemble of 5000–20000 particles was tracked to attain a reasonable trade-off between the numerical accuracy (sufficiently low statistical error) and the CPU time. During the simulation, statistics of particle motion such as mean-square dispersion and the turbulent kinetic energy were computed using the ensemble averaging.

5.1. Grid turbulence

In both S&L and W&S experiments, particle trajectories were considered in a turbulent flow behind a grid in a wind tunnel. Several particle groups of different diameter/density combinations were used; this permitted to account for the inertia effect. The particles were separately released in the flow; individual trajectories of particles were followed by an optical system and their positions were consecutively recorded by cameras placed along the tunnel. Mean-square particle displacements have been found from gathered position data. Next, the dispersion coefficients have been calculated. Fluid turbulent energy and particle kinetic energy decay were also obtained as well as the Eulerian spatial velocity correlation.

Moreover, in the second experiment (W&S), horizontal walls of the wind tunnel were two metallic chargeable plates that produced the electric field. Particles were electrically charged and the effect of the external force field was controlled by changing its intensity. This enabled to counteract the influence of gravity on particles and, in particular, to consider the particle inertia effect alone.

Figs. 11 and 12 present results of our numerical simulations (NS) using the new model presented in the previous Section; a slight modification based on the self-similarity hypothesis for grid turbulence has been introduced (for technical details, see Pozorski 1995). Moreover, to

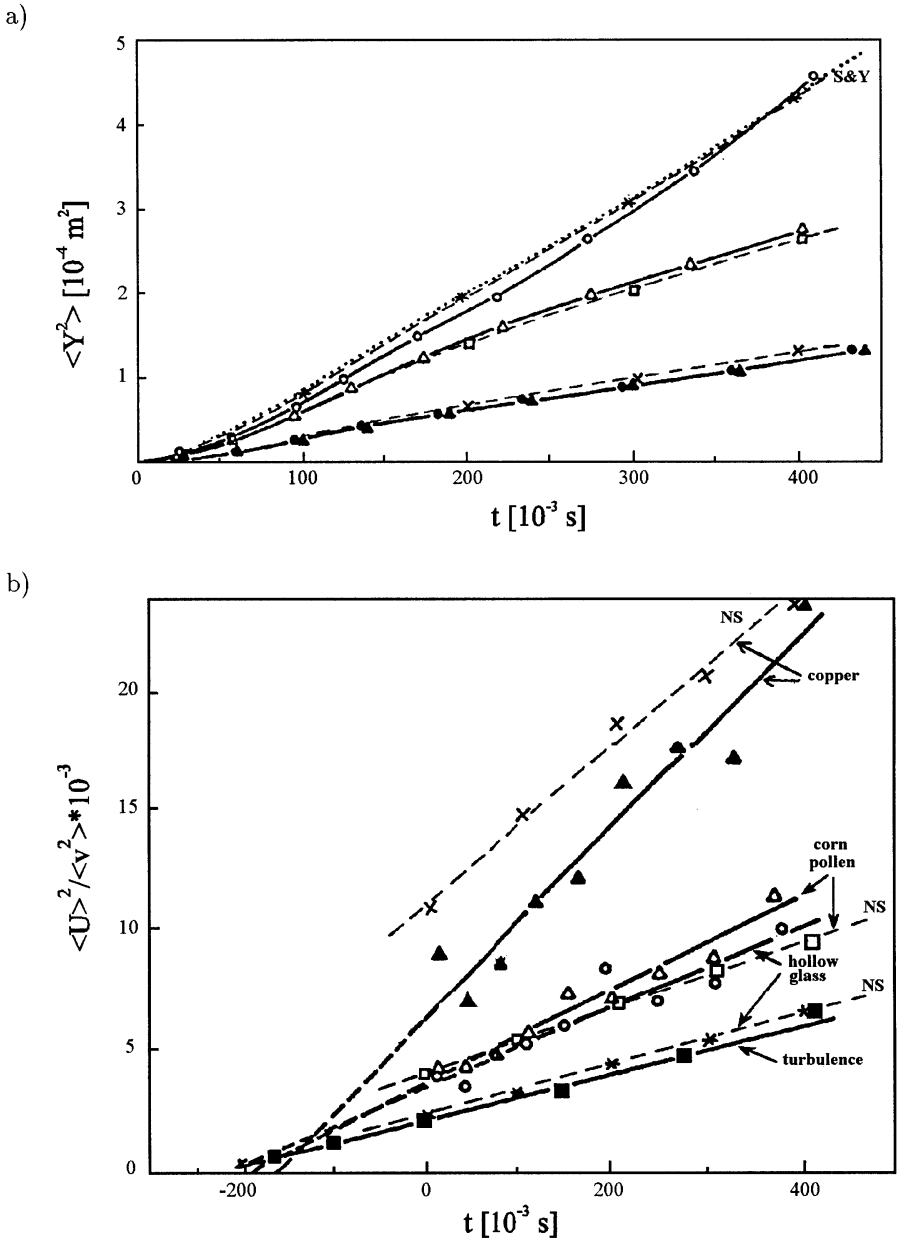

Fig. 11. Particle dispersion in grid turbulence: (a) mean-square displacement; (b) kinetic energy decay. Solid lines—experimental data (Snyder and Lumley 1971); dashed lines—numerical simulation (NS); dotted line—S&Y formula for fluid diffusion. White circles and asterisks—hollow glass, white triangles and squares—corn pollen; black triangles and crosses—copper; black squares—fluid particles.

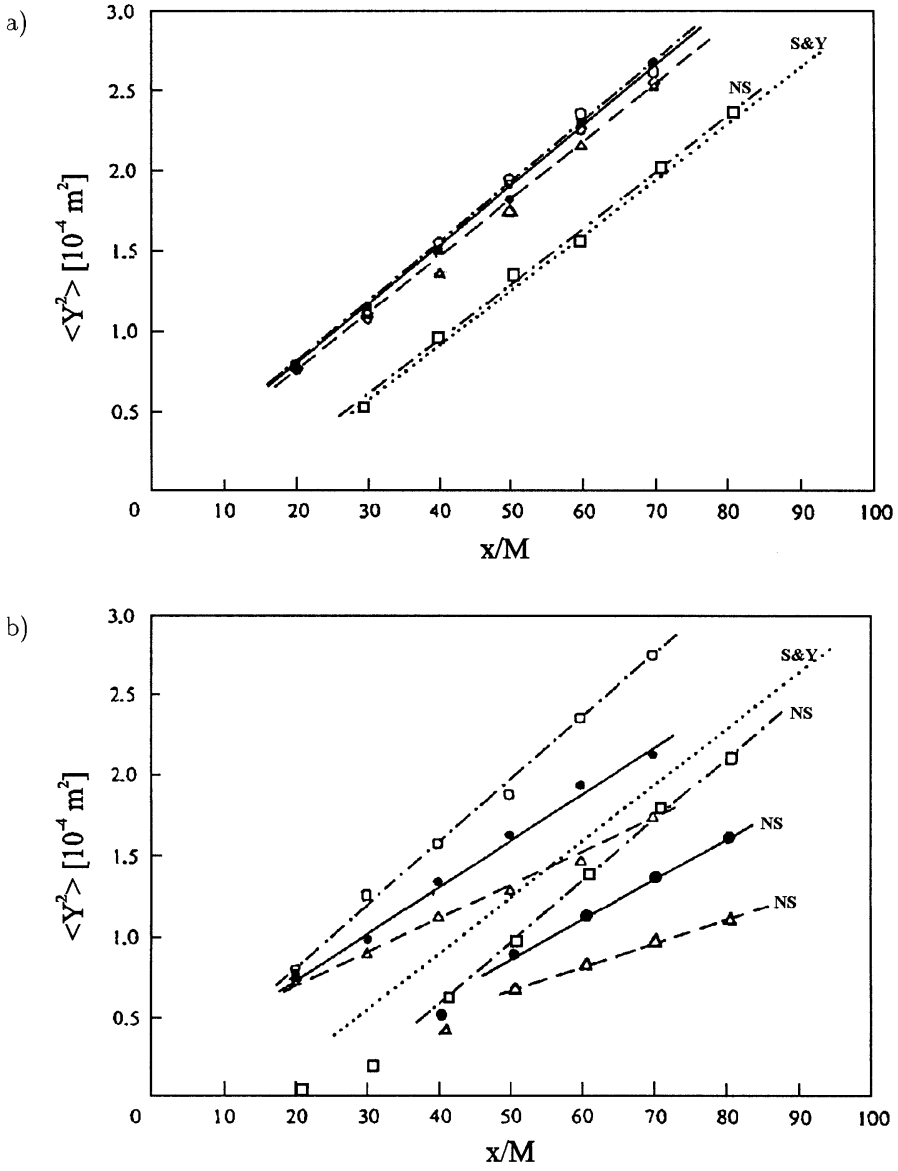

Fig. 12. Particle dispersion in grid turbulence, Wells and Stock (1983) experiment: (a) 5 μm particles; (b) 57 μm particles. Dash-dotted lines—$g = 0$; solid lines—$g = 9.81$ m/s^2, dashed lines—$g = 20.7$ m/s^2, dotted line—S&Y formula for fluid diffusion. Upper three lines are hand-fit linear approximation of the experimental data (Wells and Stock), whereas lower ones represent results of numerical simulation (NS) performed in this study. In the 5 μm particles case only one ($g = 0$) line is plotted; two others are identical.

complete the picture, a theoretical formula for fluid diffusion proposed by Sato and Yamamoto (1987), denoted as S&Y, is also shown. Results of small particle dispersion (hollow glass of S&L and 5 μm particles of W&S) are expected to stay close to those of fluid diffusion. As readily seen, the overall agreement is satisfactory.

5.2. Stationary and isotropic turbulence

Next step in evaluating numerical models for fluid diffusion and particle dispersion is the comparison of our results with those coming from LES (Deutsch, 1992) of a stationary isotropic turbulent velocity field. Its characteristics are: $\epsilon = 6.17\ \mathrm{m^2/s^3}$, $\sigma_f = 0.283$ m/s, $T_E = 0.026$ s, $T_L = 0.0233$ s, $\rho_f = 1.17\ \mathrm{kg/m^3}$. Computations have been performed for several particle diameters, $d = 15, 45, 57, 90\ \mu$m; particle density was $\rho_p = 2400\ \mathrm{kg/m^3}$.

First, the inertia effect is examined in the absence of gravity. Results of the simulations are presented in Fig. 13 together with the LES data. $T_L^*(St)$ has a characteristic 'bell-shaped' form starting from T_E (for large heavy particles when $\tau_p \to \infty$) and tending towards T_L (for small particles of $\tau_p \to 0$) as particle inertia decreases and particles follow the fluid motion more and more closely. The timescales computed from LES reach a maximum of about $1.25\ T_L$ for a particle diameter $d \approx 30\ \mu$m corresponding to a Stokes number $St = \tau_p/T_L \approx 0.3$. A possible explanation of this increase is the influence of instantaneous turbulent structures: particle locations are correlated with certain typical structures and in particular with the vorticity field. This results in longer life times of fluid structures along particle trajectories than along fluid paths and consequently in higher Lagrangian timescales T_L^* (Squires and Eaton, 1991; Deutsch, 1992). Nevertheless, to capture this effect in the Lagrangian simulation, sophisticated models using (at least) two-point correlations of the turbulent field would be needed. To the best of the authors' knowledge, none have been proposed yet.

The emergence of turbulent structures clearly represents a serious challenge for Lagrangian models. Indeed, all these models adopt a statistical point of view. Available fluid turbulent data is made up only from the statistical moments of the velocity field, since the averaging process sweeps away turbulent instantaneous structures. Furthermore, there is no reason for the statistical properties of the fluid 'seen' to be equal to the statistical properties of the

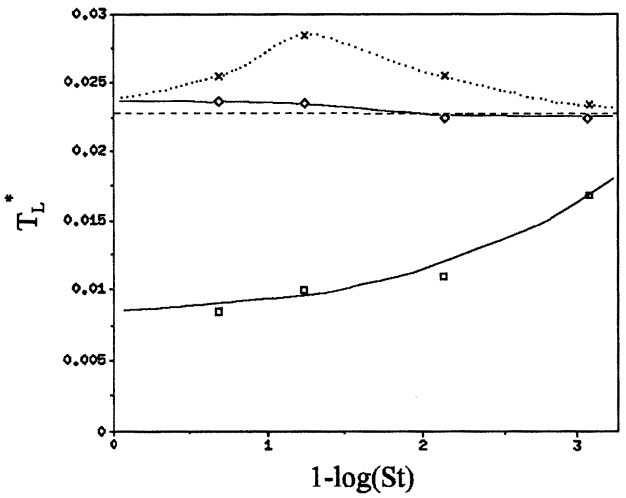

Fig. 13. Lagrangian integral timescale seen by dense particles ($d = 90, 45, 15, 5\ \mu$m from left to right) as a function of $1 - \log(St)$. The Stokes number $St = \tau_p/T_L$. Crosses—LES; diamonds—LMV model; squares—LIV model.

Eulerian velocity field. Consequently, present statistical Lagrangian models are not able to reproduce the 'bell-shaped' curve yielded by DNS and LES. On the other hand, the two asymptotic limits, T_E (for $\tau_p \to \infty$) and T_L (for $\tau_p \to 0$) should be correctly simulated. Fig. 13 shows that the integral timescale 'seen' calculated by the new model (LMV) changes from the Eulerian timescale for the largest particles to the Lagrangian timescale for the smallest ones. The result is not very easily noticed because in the present computation the value of β is close to unity, $\beta = 0.92$. As already stated at the end of Section 3, the results obtained from the instantaneous relative velocity model (LIV) are obviously in error and particularly for larger particle diameters.

The crossing trajectory effect has been thoroughly examined for three values of gravity. The simulated values of $T_L^*(\xi)/T_L^*(0)$, in directions both parallel ($\parallel$) and perpendicular ($\perp$) to gravity, are plotted in Fig. 14 for three particle diameters. Large eddy simulation results (Deutsch, 1992) are compared to Csanady's formulae (4) and two Lagrangian simulation methods: Langevin model with mean relative velocity (LMV) and its modified version, the Langevin model with mean coefficients (LMC).

The results obtained using the preliminary variant of the new model (LMV) are unsatisfactory. On the other hand, the results of its improved version (LMC) are in a good agreement with those from the LES method. Moreover, the results are close to the Csanady's formulae. We notice that both methods manifest similar asymptotic behaviour in the limits $\xi \to 0$, $\xi \to \infty$. Nevertheless, a sensitivity study (Minier and Pozorski, 1992) reveals that the methods are by no means identical and that the discrepancy between the two families of curves increases as the value of β, considered as a free parameter of the method, diminishes.

We would like to stress that our method gives $T_L^*(\xi)$ values for any ξ using the same general procedure, whereas Csanady's relations have been guessed from the known asymptotic behaviour of the space–time velocity correlation for the fluid 'seen' in the limits $\xi \to 0$, $\xi \to \infty$.

In Fig. 15, the correlation coefficients of fluid velocity 'seen' are presented for a few ξ values and $d = 90\ \mu$m. The results are relatively close to those of Deutsch, with the only exception that we are unable to reproduce negative regions in lateral velocity correlation, because of the very nature of the Langevin model.

6. Conclusion

The aim of this paper was to discuss modelling of particle dispersion in turbulent two-phase flows. We have mainly concentrated on the Lagrangian approach, considering first random-walk models for fluid elements and their generalisation for solid particles. Issues of the physical soundedness and consistency of models have been addressed. It has been stated that methods proposing straightforward extension of existing fluid diffusion models to the case of particle dispersion are not devoid of serious imperfections. A detailed analysis of an often-used Lagrangian model, i.e. the Langevin equation model with the instantaneous relative velocity (LIV), backed with the results of numerical simulations, has revealed that the model does not correctly predict neither the turbulent kinetic energy of the fluid 'seen' by the particles nor the inertia and the crossing trajectory effects.

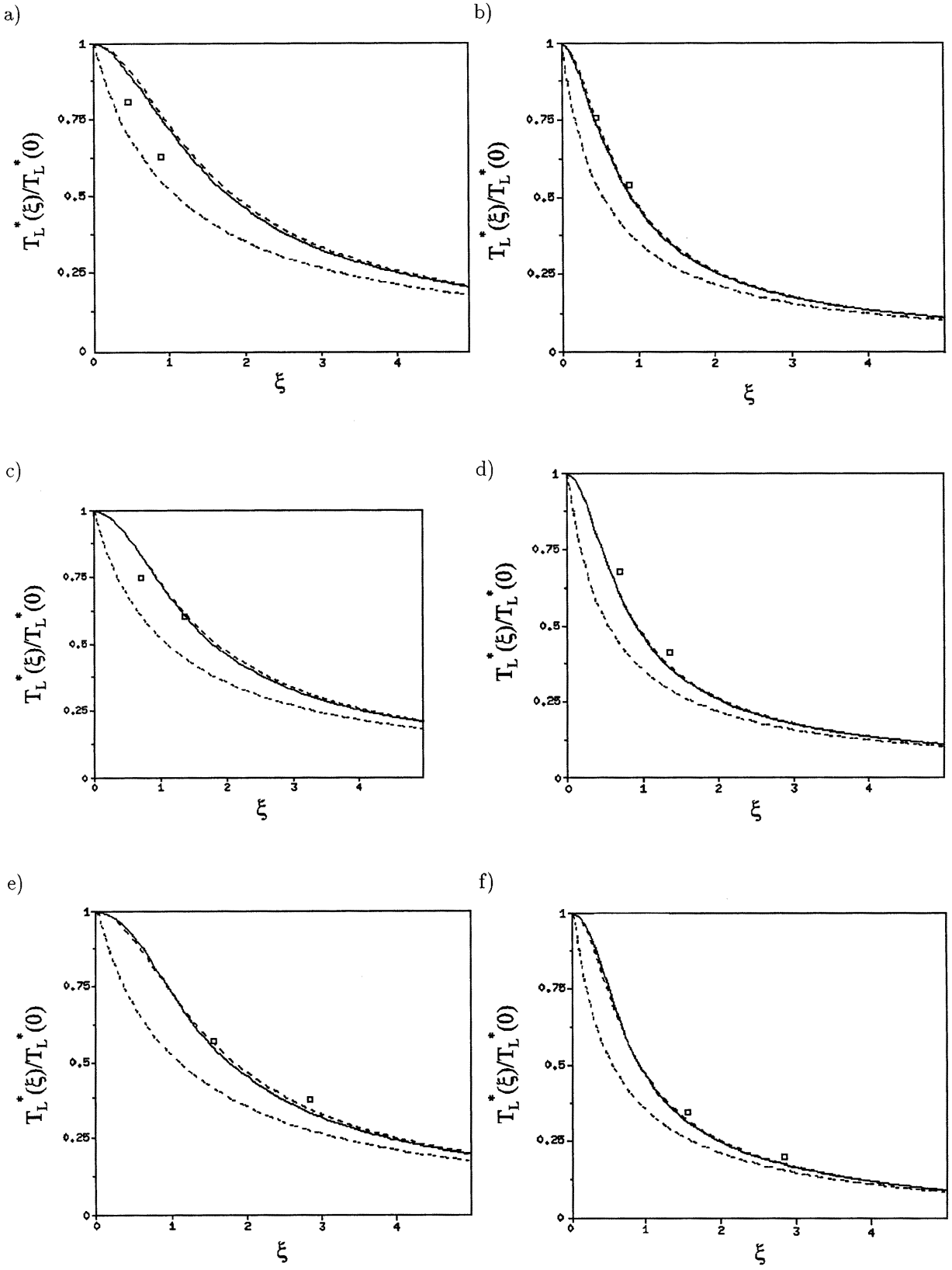

Fig. 14. Crossing trajectory effect in directions parallel (plots a,c,e) and perpendicular (plots b,d,f) to gravity: (a,b) particles $d = 45\ \mu$m; (c,d) particles $d = 57\ \mu$m; (e,f) particles $d = 90\ \mu$m. Squares—LES results; solid line—LMC; dashed line—Csanady's formulae; dot-dash line (underneath)—LMV.

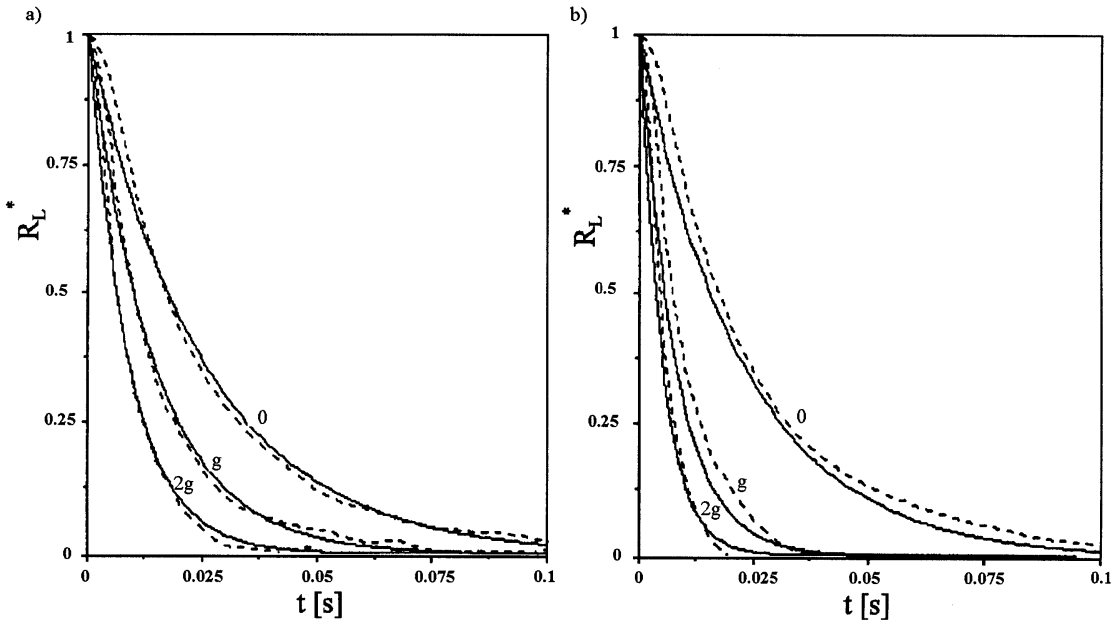

Fig. 15. Crossing trajectory effect—velocity correlations R_L^* of the fluid seen by the particles $d = 90\ \mu$m for three values of gravity: 0, g and $2g$ ($g = 9.81\ \mathrm{m/s^2}$), in directions parallel (a) and perpendicular (b) to gravity. Solid lines—LMC model; dashed lines—LES (Deutsch, 1992).

In order to account for both inertia and mean drift in a correct manner, mean behaviour of fluid–particle pairs rather than instantaneous one should be incorporated into Lagrangian dispersion models to satisfy consistency requirements. In accordance with this basic postulate, a line of reasoning has been presented that results in a new, hopefully consistent, model; it gives satisfying predictions when compared to the experimental evidence in the case of isotropic and stationary turbulence.

However, the most difficult and still uncompletely charted point is the extension of particle dispersion models to the general case of complex inhomogeneous turbulent flows, based on the experience gathered both in homogeneous particulate flows and Lagrangian modelling of fluid turbulence. At the moment, models are formulated in terms of the instantaneous fluid velocities seen by solid particles. The models follow the direct approach to particle dispersion: the timescales of the fluid seen are assumed (along Csanady's proposals) and are used in a general Langevin equation. The precise expression of the different terms remains an open question and it is hoped that the ideas put forward in the present contribution will be useful in this respect.

Although our attention has not been particularly drawn to the two-fluid approach, both Lagrangian and Eulerian description should be considered as complementary and obviously inter-related. Indeed, they use similar models and only differ in the choice of variables retained for the numerical solution. Therefore, it is hoped that progress in the fundamental understanding of inhomogeneous two-phase flow phenomena, incorporated into Lagrangian models, will ultimately result in more appropriate closure proposals in the Eulerian approach.

References

Arnold, L., 1974. Stochastic Differential Equations: Theory and Applications. Wiley, New York.

Berlemont, A., Desjonqueres, P., Gouesbet, G., 1990. Particle Lagrangian simulation in turbulent flows. International Journal of Multiphase Flow 16, 19–34.

Burry, D., Bergeles, G., 1993. Dispersion of particles in anisotropic turbulent flows. International Journal of Multiphase Flow 19, 651–664.

Clift, R., Grace, J.R., Weber, M.E., 1978. Bubbles, Drops and Particles. Academic Press, New York.

Crowe, C.T., 1982. Review—numerical models for dilute gas-particle flows. ASME Journal of Fluids Engineering 104, 297–303.

Csanady, G.T., 1963. Turbulent diffusion of heavy particles in the atmosphere. Journal of Atmospheric Science 20, 201–208.

Deutsch, E., 1992. Dispersion de particules dans une turbulence homogéne isotrope stationnaire calculée par simulation numérique directe des grandes echelles. Ph.D. thesis. Ecole Centrale de Lyon.

Durst, F., Milojevic, D., Schönung, R., 1984. Eulerian and lagrangian predictions of particulate two-phase flows: a numerical study. Applied Mathematical Modelling 8, 101–115.

Gatignol, R., 1983. The Faxén formulae for a rigid particle in an unsteady non-uniform Stokes flow. Journal de Mécanique Théorique et Appliquée 1, 143–160.

Gosman, A.D., Ioannides, E., 1981. Aspects of computer simulation of liquid-fueled combustors. 19th Aerospace Science Meeting, St Louis, MO, AIAA Paper 81-0323.

Graham, D.I., 1996. An improved eddy interaction model for numerical simulation of turbulent particle dispersion. ASME Journal of Fluids Engineering 118, 819–823.

Hinze, J.O., 1975. Turbulence. 2nd ed.. McGraw-Hill, New York.

Lu, Q.Q., Fontaine, J.R., Aubertin, G., 1993. A Lagrangian model for solid particles in turbulent flows. International Journal of Multiphase Flow 19, 347–367.

MacInnes, J.M., Bracco, F.V., 1992. Stochastic particle dispersion modeling and the tracer-particle limit. Physics of Fluids A 4, 2809–2824.

Maxey, M.R., Riley, J.J., 1983. Equation of motion for a small rigid sphere in a nonuniform flow. Physics of Fluids 26, 883–889.

Minier, J-P., Pozorski, J. 1992. Analysis of existing Lagrangian models and new propositions for particle dispersion in homogeneous stationary turbulence. Report no. HE-44/92.29, Electricité de France, Chatou.

Minier, J-P., Pozorski, J., 1997. Derivation of a PDF model for turbulent flows based on principles from statistical physics. Physics of Fluids 9, 1748–1753.

Minier, J-P., Simonin, O. 1992. A numerical approach to cyclone separators. Report no. HE-44/92.02, Electricité de France, Chatou.

Monin, A.S., Yaglom, A.M., 1971. Statistical Fluid Mechanics. MIT Press, Cambridge, MA.

Ormancey, A., 1984. Simulation du Comportement de Particules dans des Ecoulements Turbulents. Ph.D. thesis. Ecole Nationale Supérieure des Mines, Paris.

Papoulis, A., 1991. Probability, Random Variables and Stochastic Processes. 3rd ed.. McGraw-Hill, New York.

Perkins, R.J., Gosh, S., Phillips, J.C., 1991. The interaction between particles and coherent structures in a plane turbulent jet. In: A.V. Johansson, P.H. Alfredsson (Ed.). Advances in Turbulence 3. Springer, Berlin.

Pope, S.B., 1994. Lagrangian modeling of turbulent flows. Annual Review of Fluid Mechanics 26, 23–63.

Pozorski, J., 1995. Numerical simulation of dispersed phase motion in turbulent two-phase flow. Doctoral thesis, Instytut Maszyn Przeplywowych PAN (Institute of Fluid-Flow Machinery, Polish Academy of Sciences), Gdańsk.

Pozorski, J., Minier, J-P., Simonin, O., 1993. Analysis and new propositions for the crossing-trajectory effect in Lagrangian turbulent dispersion models. In: Gas-Solid Flows, ASME FED 166, 63–71.

Saffman, P.G., 1963. An approximate calculation of the Lagrangian auto-correlation coefficient for stationary homogeneous turbulence. Applied Science Research A 11, 447–459.

Sato, Y., Yamamoto, K., 1987. Lagrangian measurement of fluid–particle motion in an isotropic turbulent field. Journal of Fluid Mechanics 175, 183–199.

Schuss, Z., 1980. Theory and Applications of Stochastic Differential Equations. Wiley, New York.

Simonin, O. 1996. Eulerian numerical approach for prediction of gas–solid turbulent two-phase flows. Von Karman Institute Lecture Series. 1996-02, Rhode-Saint-Genese, Belgium.

Simonin, O., Deutsch, E., Minier, J-P., 1993. Eulerian prediction of the fluid/particle correlated motion in turbulent two-phase flows. Applied Science Research 51, 275–283.

Snyder, W.H., Lumley, J.L., 1971. Some measurements of particle velocity autocorrelation functions in a turbulent flow. Journal of Fluid Mechanics 48, 41–71.

Sobczyk, K., 1991. Stochastic Differential Equations with Applications to Physics and Engineering. Kluwer Academic, New York.

Sommerfeld, M., Kohnen, G., Rüger, M. 1993. Some open questions and inconsistencies of Lagrangian particle dispersion models. 9th Symposium on Turbulent Shear Flows. Kyoto, Japan.

Squires, K.D., Eaton, J.K., 1991. Preferential concentration of particles by turbulence. Physics of Fluids A 3, 1169–1178.

Stock, D.E., 1996. Particle dispersion in flowing gases. ASME Journal of Fluids Engineering 118, 4–17.
Wells, M.R., Stock, D.E., 1983. The effect of crossing trajectories on the dispersion of particles in a turbulent flow. Journal of Fluid Mechanics 136, 31–62.
Yvergniaux, P., 1990. Simulation Euléro–Lagrangienne du transport de particules solides en suspension dans un ecoulement turbulent en canal. Ph.D. thesis, Institut National Polytechnique de Grenoble.
Zhou, Q., Leschziner, M.A., 1991. A Lagrangian particle dispersion model based on a time-correlated stochastic approach. In: Gas–Solid Flows, ASME FED Vol. 121, 255–260.
Zhuang, Y., Wilson, J.D., Lozowski, E.P., 1989. A trajectory simulation model for heavy particle motion in turbulent flow. ASME Journal of Fluids Engineering 111, 492–494.